Translational Oncology
www.transonc.com

Volume 7 Number 2 April 2014 pp. 174–187.e5 174

Urokinase-Type Plasminogen Activator Deficiency Promotes Neoplasmatogenesis in the Colon of Mice[1,2,3]

Elisavet Karamanavi*, Katerina Angelopoulou†, Sophia Lavrentiadou‡, Anastasia Tsingotjidou§, Zaphiris Abas¶,4, Ioannis Taitzoglou‡, Ioannis Vlemmas*, Suzan E. Erdman# and Theofilos Poutahidis*

*Laboratory of Pathology, Faculty of Veterinary Medicine, Aristotle University of Thessaloniki, Thessaloniki, Greece; †Laboratory of Biochemistry and Toxicology, Faculty of Veterinary Medicine, Aristotle University of Thessaloniki, Thessaloniki, Greece; ‡Laboratory of Physiology, Faculty of Veterinary Medicine, Aristotle University of Thessaloniki, Thessaloniki, Greece; §Laboratory of Anatomy, Histology and Embryology, Faculty of Veterinary Medicine, Aristotle University of Thessaloniki, Thessaloniki, Greece; ¶Department of Agricultural Development, Democritus University of Thrace, Orestiada, Greece; #Division of Comparative Medicine, Massachusetts Institute of Technology, Cambridge, MA, USA

Abstract

Urokinase-type plasminogen activator (uPA) participates in cancer-related biologic processes, such as wound healing and inflammation. The present study aimed to investigate the effect of uPA deficiency on the long-term outcome of early life episodes of dextran sodium sulfate (DSS)–induced colitis in mice. Wild-type (WT) and uPA-deficient ($uPA^{-/-}$) BALB/c mice were treated with DSS or remained untreated. Mice were necropsied either 1 week or 7 months after DSS treatment. Colon samples were analyzed by histopathology, immunohistochemistry, ELISA, and real-time polymerase chain reaction. At 7 months, with no colitis evident, half of the $uPA^{-/-}$ mice had large colonic polypoid adenomas, whereas WT mice did not. One week after DSS treatment, there were typical DSS-induced colitis lesions in both WT and $uPA^{-/-}$ mice. The affected colon of $uPA^{-/-}$ mice, however, had features of delayed ulcer re-epithelialization and dysplastic lesions of higher grade developing on the basis of a significantly altered mucosal inflammatory milieu. The later was characterized by more neutrophils and macrophages, less regulatory T cells (Treg), significantly upregulated cytokines, including interleukin-6 (IL-6), IL-17, tumor necrosis factor-α, and IL-10, and lower levels of active transforming growth factor–β1 (TGF-β1) compared to WT mice. Dysfunctional Treg, more robust protumorigenic inflammatory events, and an inherited inability to produce adequate amounts of extracellular active TGF-β1 due to uPA deficiency are interlinked as probable explanations for the inflammatory-induced neoplasmatogenesis in the colon of $uPA^{-/-}$ mice.

Translational Oncology (2014) 7, 174–187.e5

Address all correspondence to: Theofilos Poutahidis, Laboratory of Pathology, Faculty of Veterinary Medicine, Aristotle University of Thessaloniki, Thessaloniki 54124, Greece.
E-mail: teoput@vet.auth.gr

[1] This study is dedicated to the memory of Dr. Zaphiris Abas.

[2] This work was supported in part by National Institutes of Health grant RO1CA108854 (to S.E.E.).

[3] This article refers to supplementary materials, which are designated by Tables W1 and W2 and Figures W1 to W4 and are available online at http://www.transonc.com.

[4] Deceased.

Received 28 October 2013; Revised 14 January 2014; Accepted 15 January 2014

 1936-5233/14
http://dx.doi.org/10.1016/j.tranon.2014.02.002

Introduction

Accumulating evidence suggests that cells and factors of the tumor microenvironment contribute decisively not only to the survival of primary neoplastic cells but also to subsequent key events of neoplastic disease progression including tumor growth, invasion, and metastasis [1-3]. Various and many times interrelated determinants govern this complex tumor-host interaction; among them inflammatory and proteolytic-related phenomena have been shown to be particularly important [4-8]. It is now well accepted that chronic inflammation may lead to tumorigenesis [4,7,9]. Several lines of evidence, however, show that all neoplasms, not just those arising on the background of chronic inflammation, thrive with inflammatory cell stimuli. Indeed, many times the tumor elicited immune response is unable to eliminate a rapidly growing population of cells that is always one step ahead due to the natural selection advantage. Instead, it shapes the tumor stroma in favor of cancer cell survival and expansion in a manner similar to that observed in tissue remodeling and repair [2,3,6,7]. In that sense, the view of cancer as "a wound that does not heal" [10] has been further solidified. Consequently, key regulators of wound healing, such as immune cells and proteases, are now recognized as fundamental rather than secondary players in neoplasmatogenesis [3].

One such regulator is urokinase-type plasminogen activator (uPA), a protease that has a dominant role in the proteolytic network and is primarily involved in fibrinolysis, tissue remodeling, and cell migration [11-14]. uPA catalyzes the conversion of plasminogen to plasmin and also activates other important proteases, including cathepsin B and matrix metalloproteinases. The targets of uPA in turn activate an array of proteins with a broad spectrum of biologic activities [13,14]. In the tumor microenvironment, the complex cascades initiated by uPA promote tumor progression. First, they facilitate neoplastic cell invasion, motility, and metastasis by degrading epithelial basement membranes and the extracellular matrix. Second, they support tumor growth by stroma remodeling and angiogenesis. Finally, they are involved in proliferating and antiapoptotic tumor cell signaling [8,14-18]. These facts, supported by many studies in both animal models [19-24] and humans [15,25], have placed uPA among the tumor promoting molecules with emerging importance. To date, uPA is considered as a poor prognosis factor and a potential therapeutic target for most types of cancer including colorectal cancer [15,25,26].

Transforming growth factor–β1 (TGF-β1) is one of the most important factors activated by the uPA-generated plasmin [14,27]. TGF-β1 is ubiquitously produced by a variety of cells and excreted in the extracellular matrix in a latent form. The cleavage of this form by plasmin results in the production of the biologically active TGF-β1 [28], which has been shown to act as a tumor suppressor in the early stages of tumor development and as a major regulator of immune events in the tumor microenvironment [29,30]. As with the corruption of normal TGF-β1 signaling pathways at the gene level [29,30], the lack of extracellular active TGF-β1 protein may also increase the risk of cancer initiation. Following this reasoning, we hypothesized that uPA and TGF-β1 may have an interlinked tumor-suppressive function. This, however, contradicts with the current view of uPA as a tumor promoting molecule [8,15-18].

To investigate our hypothesis, we examined the effect of uPA deficiency on the outcome of transient episodes of dextran sodium sulfate (DSS)–induced colitis in BALB/c mice. The DSS administration protocol we used leads neither to overt chronic colitis nor to colon cancer when applied to genetically intact BALB/c mice. However, it does lead to the induction of preneoplastic epithelial changes [31]. Using this experimental setting, we found that the mice lacking uPA, in contrast to their wild-type (WT) counterparts, were predisposed to adenomatous polyp formation. The colonic epithelial preneoplasia in these mice evolved into adenomatous polyps on the basis of a significantly altered mucosal inflammatory milieu, which was characterized by more neutrophils and macrophages, less regulatory T cells (Treg), significantly upregulated cytokines, including interleukin-6 (IL-6), IL-17, tumor necrosis factor-α (TNF-α), and IL-10, and lower levels of active TGF-β1. Our results challenge the dogma according to which uPA is viewed solely as a tumor promoter.

Materials and Methods

Animals

Specific pathogen-free certified C.129S2-Plau<tm1Mlg>/J uPA-deficient ($uPA^{-/-}$) mice and background strain-matched control BALB/cJ WT mice were purchased from Jackson Laboratories (Bar Harbor, ME) and bred in-house to provide animals for the experiments. Mice were kept in bio-containment facilities in static micro-isolator cages, fed with sterilized regular mouse chow, and given sterilized water. *Helicobacter*-free status of the mice was confirmed by polymerase chain reaction (PCR) using *Helicobacter* genus–specific primers in fecal and gut mucosa samples as previously described [32]. All experimental procedures were approved by the Faculty of Veterinary Medicine, Aristotle University of Thessaloniki and licensed by the competent National Veterinary Administration authorities (License No. 13/11197/11.09.08).

Experimental Design

A total of 130 (66 $uPA^{-/-}$ and 64 WT) male mice were used. Experiments were performed in three replications to achieve a total number of 11 to 24 mice per experimental group. For the induction of chronic colitis, 3.5% DSS (molecular weight: 36-50 kDa; MP Biomedicals Inc, Cleveland, OH) was given in the drinking water of 8- to 10-week-old mice for 1 week followed by 1 week of regular water. This cycle was repeated three times. $uPA^{-/-}$ and WT mice were either treated with DSS or remained untreated. Mice were killed either at 7 months (first experiment—long term) or at 1 week (second experiment—short term) after DSS treatment. Numbers of mice per experimental group for each experiment were as follows: *first experiment*: $uPA^{-/-}$ (n = 11), WT (n = 11), $uPA^{-/-}$ + DSS (n = 11), WT + DSS (n = 11); *second experiment*: $uPA^{-/-}$ (n = 20), WT (n = 19), $uPA^{-/-}$ + DSS (n = 24), WT + DSS (n = 23).

Necropsy and Tissue Sampling

Mice were killed with an overdose of isoflurane, weighted, and necropsied. The colon of mice was then removed and cut open, and the mucosal surface was photographed in high resolution for grossly visible polypoid adenoma counts. One-centimeter colon samples were collected from a standard area of the proximal part of descending colon for gene expression and ELISA analyses. Samples for gene expression assay were immediately immersed in an RNA-later solution (Takara Bio Inc, Shiga, Japan) and stored at −80°C until further processing. The remaining colon was fixed in 10% neutral-buffered formalin for histologic and immunohistochemical analyses.

Histopathology, Immunohistochemistry, and Morphometry

For histologic evaluation, formalin-fixed colon and mesenteric lymph nodes (MLN) were embedded in paraffin, cut at 5 μm, and stained with hematoxylin and eosin or immunohistochemistry (IHC). Dysplastic and neoplastic lesions in the colonic mucosa (excluding polyps) were scored on a 0 to 4 ascending scale using previously described criteria [33]. Mucosal/submucosal inflammation in the colon was scored in non-ulcerated areas based on the extent and severity of inflammatory cell accumulations. Loss of colonic epithelial integrity was scored on the basis of the extent and severity of the typical DSS-induced colonic mucosal erosive and ulcerative lesions. Both parameters were scored semi-quantitatively on 0 to 4 ascending scales according to the following scheme: 0, normal; 1, mild; 2, mild to moderate; 3, moderate; 4, severe.

Primary antibodies for IHC included 1) rabbit polyclonal antibodies against β-catenin, myeloperoxidase (MPO; Thermo Fisher Scientific/Lab Vision, Fremont, CA), E-cadherin, IL-17, TGF-β1 (Santa Cruz Biotechnology, Inc, Santa Cruz, CA), cleaved caspase-3 (Cell Signaling Technology, Beverly, MA), and CD3 (Cell Marque, Rocklin, CA); 2) rabbit monoclonal antibodies against Ki-67 and c-kit (Cell Marque); 3) rat monoclonal antibodies against Foxp3 (eBioscience, Inc, San Diego, CA) and F4/80 (Serotec, Oxford, United Kingdom); and 4) a goat polyclonal antibody against IL-16 (Santa Cruz Biotechnology, Inc). Heat-induced antigen retrieval was performed with citrate buffer, pH 6, for β-catenin, E-cadherin, MPO, and cleaved caspase-3, with EDTA buffer, pH 8, for IL-17 and Foxp-3, or with CC1 epitope retrieval solution for Ki-67, CD3, and IL-6 (Ventana Medical Systems, Inc, Tucson, AZ). TGF-β1 antigens were retrieved with protease (Cell Marque) and F4/80 antigens with trypsin (Thermo Fisher Scientific/Lab Vision). Rabbit primary antibody binding was detected with goat anti-rabbit polymer HRP (ZytoChem Plus, Berlin, Germany), whereas rat and goat primary antibody binding was detected with species-appropriate biotinylated secondary antibodies (Serotec) and streptavidin-peroxidase (Ventana Medical Systems, Inc). Color was developed with DAB substrate-chromogen system (DakoCytomation, Glostrup, Denmark), and tissues were counterstained with hematoxylin.

For quantitative histomorphometry, IHC-positive immune cells or pixels were counted in images of ×20 or ×40 representative high power fields as previously described [34], and results were recorded as number of cells or pixels per image. The ImageJ image processing and analysis program (National Institutes of Health, Bethesda, MD) was used for all quantitative histomorphometry assessments.

Enzyme-Linked Immunosorbent Assay

For protein extraction, 50 mg of tissue was homogenized using a motor-driven homogenizer (Kinematica AG, Luzern, Switzerland) in a 500-μl solution containing 1× phosphate-buffered saline and 1× protease inhibitor cocktail (Sigma-Aldrich Chemie GmbH, Taufkirchen, Germany). The homogenate was centrifuged at 12,000 rpm for 20 minutes, at 4°C. The supernatant was collected and used for further analysis. Total protein in tissue extracts was measured using the BCA Protein Assay Kit (Thermo Scientific, Rockford, IL). The concentrations of uPA and active TGF-β1 in tissue extracts were determined using the commercial ELISA kits Mouse uPA Activity Assay kit (Innovative Research, Novi, MI) and TGF-β1 E_{max} ImmunoAssay System (Promega Corporation, Madison, WI), respectively. Manufacturers' instructions were followed throughout. Absorbance was measured at 450 nm on an ELISA plate reader (STAT FAX 2100; Awareness Technology, Inc, Palm City, FL).

Quantitative Gene Expression Analysis

Total RNA was extracted from tissue samples using the NucleoSpin Total RNA Isolation kit (Macherey-Nagel, Duren, Germany) according to the manufacturer's instructions. After spectrophotometric determination of RNA concentration and quality, samples were stored at −80°C until use. Reverse transcription was carried out using the PrimeScript 1st strand cDNA synthesis kit (Takara); manufacturer's instructions were followed throughout. One microgram of total RNA was used as starting material for cDNA synthesis. Real-time PCR based on the SYBR Green chemistry was used to quantitatively analyze the expression of *TNF-α*, *IL-6*, *IL-10*, *TGF-β1*, *SMAD4*, and *TGF-β receptor type II* (*TGF-βRII*). The housekeeping gene *glyceraldehyde-3-phosphate dehydrogenase* (*GAPDH*) was used as an internal control. Primers were designed using the Primer3 Input software (version 0.4.0), according to nucleotide sequences available in GenBank (Accession Nos.—*TNF-α*: NM_013693, *IL-6*: NM_031168, *IL-10*: NM_010548, *TGF-β1*: NM_011577, *SMAD4*: NM_008540, *TGF-βRII*: NM_009371, *GAPDH*: NM_008084). Primer sequences, their positions within the corresponding genes, and amplicon sizes are presented in Table W1. PCR amplification was performed in 20-μl reaction mixtures containing 2 μl of cDNA, 1× KAPA SYBR FAST qPCR master mix (KAPA BIOSYSTEMS, Woburn, MA), and 150 to 300 nM of each primer pair (Table W2). The temperature cycling on a Bio-Rad MiniOpticon System (Bio-Rad Laboratories, Hercules, CA) included 40 cycles consisting of denaturation at 95°C for 10 seconds and annealing/extension at temperatures ranging from 57 to 63°C for 20 seconds (Table W2). Each PCR reaction was initiated with a 3-minute denaturation at 95°C and terminated with sequential readings between 65 and 95°C (increment of 0.5°C) to generate the melting curve and verify amplicon specificity. For relative quantification of gene expression, we used the comparative C_T method, also known as the $2^{-\Delta\Delta CT}$ method [35].

Statistical Analyses

Adenomatous polyp counts were analyzed by the Kruskal-Wallis one-way analysis of variance and Dunn's post-test. Histomorphometry, relative gene expression, and protein quantification data were compared between groups using Mann-Whitney *U* analysis. Statistical significance was set at $P < .05$. All analyses were performed with the GraphPad Prism version 5.0 for windows (GraphPad Software, San Diego, CA).

Results

At 7 Months after DSS Treatment, uPA$^{-/-}$ Mice Develop Large Sporadic Colorectal Polyps

On necropsy, 7 months after the last episode of experimentally induced colitis, the only difference observed between experimental groups was that DSS-treated mice had prominently larger MLN compared to the untreated controls. When the intestines were cut open, however, in 5 of the 11 mice, 7 grossly visible, well-sized polyps were found (Figure W1*A*). The colonic mucosa exophytic tumors, which had the typical cornflower-like appearance of colonic polypoid adenomas (Figure 1*A*), had sizes ranging from 2 to 10 mm in diameter and were located either in the descending colon (five of seven) or in the rectum

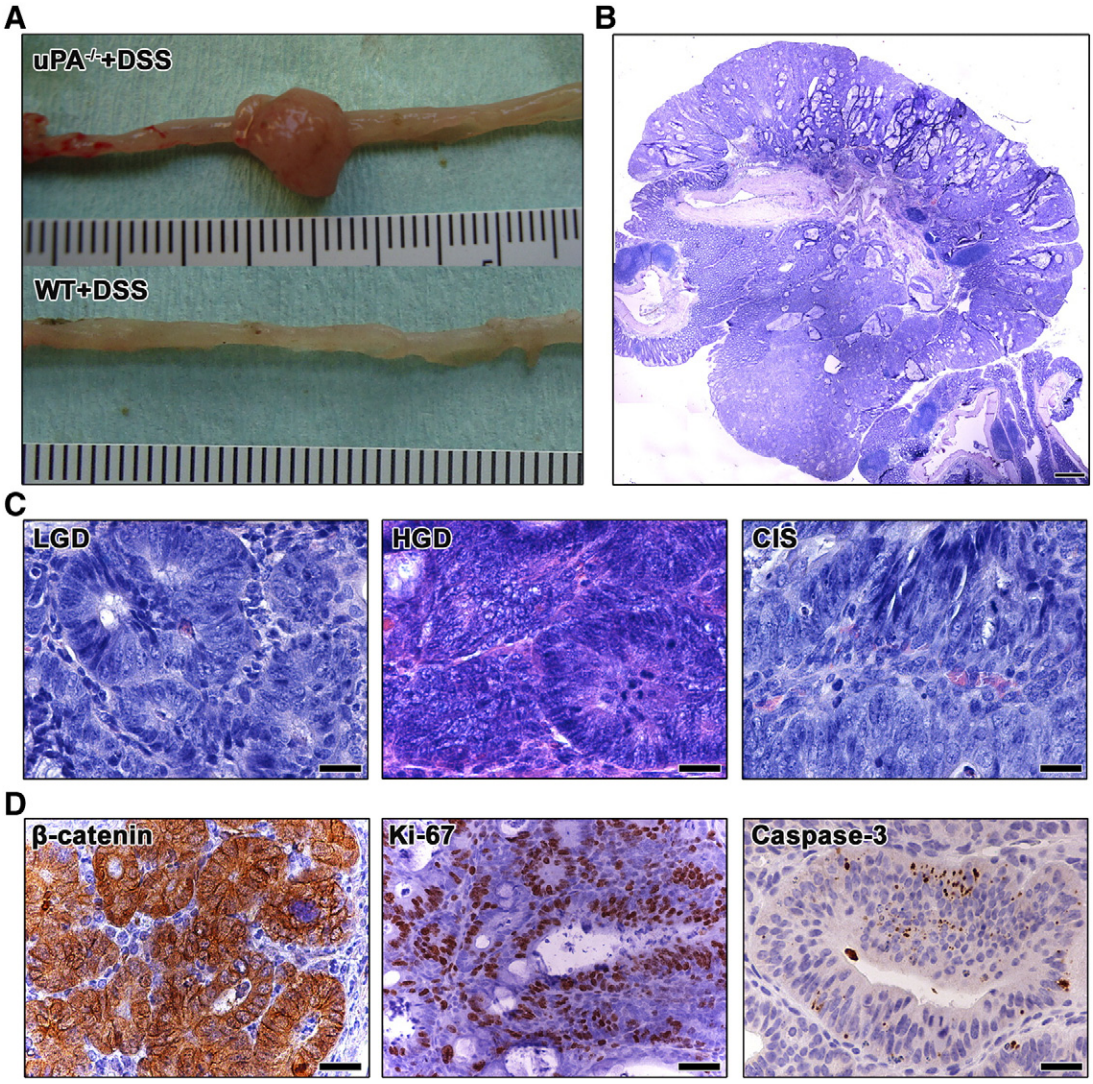

Figure 1. Pathologic features of uPA$^{-/-}$ + DSS–treated mouse colorectal polypoid adenomas. (A) Gross pathology of a well-formed colonic polyp found in the descending colon of a uPA$^{-/-}$ + DSS mouse. Normal colon from a WT + DSS mouse is shown below for comparison. The metric scale included in the images is in centimeters. (B) Overview of a uPA$^{-/-}$ + DSS colonic polyp presenting typical histopathologic features of tubular adenoma with dense tubular abnormal gland arrangement and cystically dilated mucin-filled glands. (C) Histomorphologic grading of dysplasia/adenoma lesions contained in polyps. The progression from low-grade dysplasia/adenoma to high-grade dysplasia/adenoma and CIS is characterized by progressively increased severity of indices of dysplasia including glandular shape and size irregularities, epithelial pseudostratification, cellular atypia, nuclear size, and pleomorphism and mitotic figures. (D) Characteristic immunohistochemical features of polypoid adenomas. There is abnormal β-catenin cytoplasmic stabilization with occasional nuclear translocation. Abnormal epithelia show numerous Ki-67–positive proliferating cells and increased apoptosis highlighted by caspase-3 labeling. Hematoxylin and eosin (B and C). IHC: DAB chromogen, hematoxylin counterstain (D). Scale bars, 1500 μm (B); 25 μm (C and D; β-catenin and caspase-3); 50 μm (D; Ki-67).

(two of seven). The surface of the largest four polyps (four of seven) had erosions and microhemorrhages. No grossly detectable polyps were found in the intestines of uPA$^{-/-}$, WT, and WT + DSS experimental groups (uPA$^{-/-}$ + DSS polyps = 7 *vs* WT + DSS polyps = 0, $P < .05$; Figure 1*A*). This finding suggested that uPA$^{-/-}$ + DSS mice could model sporadic colorectal polypoid adenomas of humans. To confirm this, we next characterized the histopathologic and selected immunohistochemical features of inflammation-induced polyps.

Histopathologic and Immunohistochemical Characterization of uPA$^{-/-}$ + DSS Mice Colorectal Polyps

The DSS-induced colorectal polyps of uPA$^{-/-}$ mice had the typical histopathologic features of colorectal polypoid adenomas that arise spontaneously in humans or after chemically induced carcinogenesis in mouse models (Figure 1*B*). All of them were tubular adenomas. Four of them were broad-based (four of seven) and three were pedunculated (three of seven). The tumors composed of elongated, branching, tortuous abnormal crypts, separated by small amounts of intervening stroma (Figure 1*B*). Neoplastic gland profiles were densely packed, with back-to-back positioning and had irregular shape, which was often angular. They also showed marked variability in shape and size, slit-shaped lumen, and cystic dilatation (Figures 1, *B* and *C*, and S1*B*). Occasional dilated crypts were filled with mucin and exfoliated cells. The neoplastic glands were lined by highly dysplastic epithelium showing moderate to marked pseudostratification, loss of nuclear polarity, cellular pleomorphism, and atypia

(Figures 1*C* and W1, *B* and *C*). Mitotic figures, including abnormal ones (Figure W1*C*), were abundant (Figures 1, *C* and *D*, and W1, *B* and *C*), whereas the most advanced lesions contained increased apoptotic cells (Figure 1*D*). On the basis of previously published histomorphologic criteria, foci of dysplasia/adenoma lesions within polyps were identified as low-grade dysplasia (LGD) or high-grade dysplasia (HGD) and carcinoma *in situ* (CIS, intraepithelial neoplasia; Figure 1*C*). All polyps (seven of seven) contained neoplastic gland foci staged as LGD and HGD. Four polyps also contained CIS lesions (four of seven). No polyp (zero of seven) contained early invasive adenocarcinoma lesions, such as neoplastic gland invasion into the polyp stalk or the underlying submucosa.

Immunohistochemically, the polyps showed abnormal β-catenin (Figures 1*D* and W1*D*) and E-cadherin (Figure W1*D*) patterns, with loss of normal cell membrane localization and cytoplasmic stabilization. Neoplastic glands with CIS lesions also had epithelial cells with nuclear translocation of β-catenin. TGF-β1 expression within polyps had no specific pattern. Areas of normal, increased, and decreased expression co-existed (Figure W1*D*). LGD and HGD lesions, however, most often were overexpressing TGF-β1, whereas occasional HGD and CIS lesions showed a decreased or a complete loss of positive immunolabeling. The proliferation and apoptosis was typical for polypoid adenomas with Ki-67– and caspase-3–positive neoplastic cells being more abundant in HGD and CIS lesions (Figure 1*D*).

Distribution of Inflammatory Cells within Polyps

To further characterize the uPA$^{-/-}$ + DSS mouse model of colorectal neoplasia, we next examined the topographic distribution of inflammatory cells in the polyps. The major part of the tumor-associated inflammatory cell infiltrate located in the lamina propria overlying the muscularis mucosa and the submucosa layer at the base of the polyp (Figure W2*A*). Secondarily, inflammatory cells accumulated in the lamina propria below the surface epithelium of the polyp and the non-neoplastic epithelium at the peripheral margins of the polyp. Less inflammatory cells were seen within the tumor stroma of the main body of the polyps. At the base of the polyp, the infiltrate consisted of lymphocytes, neutrophils, macrophages, mast cells, myeloid precursor cells, and plasmacytes (Figure W2*A*). Subepithelially, there were mainly macrophages, neutrophils, and fewer lymphocytes, whereas at the tumor margins there were macrophages, lymphocytes, and less neutrophils and plasmacytes. Within the main body of the tumors, there were neutrophils, macrophages, and occasional lymphocytes.

The immunohistochemical labeling of selected immune cells and cytokines confirmed the above-mentioned histologic observations (Figure W2, *B*–*H*). The main body of the polyp was infiltrated primarily by MPO+ neutrophils (Figure W2*B*) and, to a lesser extent, by F4/80+ macrophages. At the base of the polyp, there were numerous MPO+, F4/80+ (Figure W2*C*), and CD3+ (Figure W2*D*) cells. CD3+ T-lymphocytes and Foxp3+ Treg confined at the periphery of the polyp (Figure W2*E*) and rarely located between neoplastic glands, whereas c-kit+ mast cells were almost exclusively found at the base of the polyp and the underlying submucosa and muscle layers (Figure W2*F*). The main sources of IL-17 and IL-6 in the tumor microenvironment were inflammatory cells located at the base of the polyp. Specifically, there were IL-6+ macrophages and neutrophils (Figure W2*G*) and IL-17+ macrophages and lymphocytes (Figure W2*H*).

At 7 Months after DSS Treatment, the Occurrence and Severity of Epithelial Dysplasia Is Higher in the Colon of uPA$^{-/-}$ Mice

In addition to the development of polyps, the remaining non-polypoid colonic epithelium of uPA$^{-/-}$ + DSS mice was given a significantly higher score for dysplasia compared to WT + DSS mice ($P = .0006$). Two of 11 WT + DSS mice had occasional foci of mild dysplasia, whereas 10 of 11 uPA$^{-/-}$ + DSS mice showed foci of both mild dysplasia and LGD lesions in their colonic mucosa (excluding polyps; Figure 2*A*). The histopathologic and immunohistochemical characteristics of non-polypoid epithelial dysplastic lesions were similar to their grade-match counterparts found in the polyps. Similarly to WT control mice, uPA$^{-/-}$ controls had no dysplastic lesions in their bowel, indicating that in the absence of inflammatory stimuli, the deficiency of *uPA* is not sufficient for colonic neoplasmatogenesis (Figure 2*A*).

At 7 Months after DSS Treatment, the Colon of uPA$^{-/-}$ Mice Has More Resident Inflammatory Cells

Seven months after the last cycle of DSS treatment, 5 of 11 uPA$^{-/-}$ + DSS mice showed a small-sized solitary residual ulcerative lesion in the last part of the descending colon or in the rectum. This lesion was absent from WT + DSS mice (0 of 11; Figure W3*A*). Otherwise, the colon of both DSS-treated groups had no signs of remaining colitis. However, the histopathologic score for the presence of resident inflammatory cells in the colonic mucosa and submucosa (excluding polyp, dysplastic, and solitary residual ulcerative colitis areas) was significantly higher in uPA$^{-/-}$ + DSS mice compared to that of WT + DSS mice ($P = .0454$; Figure 2*A*). The uPA$^{-/-}$ and WT untreated control groups had comparable numbers of colonic resident inflammatory cells (Figure 2*A*). Taken together, these results indicate that 7 months after the DSS-induced episodes of colitis, uPA$^{-/-}$ mice fail to reduce the numbers of colonic inflammatory cells, as close to the untreated control baseline levels, as their WT counterparts. In addition, uPA deficiency alone, in the absence of colitogenic stimuli, does not affect residential colonic inflammatory cells. To quantify more accurately this result, we next performed morphometric counts of immunohistochemically labeled immune cells. We found that uPA$^{-/-}$ + DSS mice had significantly more MPO+ neutrophils ($P = .0002$; Figure 2*B*), F4/80+ macrophages ($P = .0008$; Figure 2*B*), IL-6+ ($P = .0015$; Figure W3*B*), and IL-17+ ($P = .0009$; Figure W3*B*) cells in the colon and significantly more Foxp3+ Treg in the colon ($P = .0046$; Figure 2*B*) and the MLN ($P = .0185$; Figure W3*C*) compared to WT + DSS mice. By contrast, the total number of CD3+ T-helper lymphocytes was higher in the colon of WT + DSS mice reaching, however, no statistical significance ($P = .0818$; Figure W3*B*). The presence of c-kit+ mast cells was unremarkable in both groups. By comparison to untreated uPA$^{-/-}$ controls, uPA$^{-/-}$ + DSS mice had significantly higher numbers of both innate and adaptive immunity cells (Figure 2*B*). At the same time, residual colonic innate immunity cells, such as neutrophils and macrophages, of WT + DSS mice regressed to WT control baseline levels (Figure 2*B*). The adaptive immunity colonic mucosa cells, including Treg, however, did not fully regress (WT *vs* WT + DSS, $P = .048$; Figure 2*B*). This result, which is in line with gross pathology observation of MLN enlargement at 7 months after DSS treatments, suggests that subtle alterations in local gut adaptive immunity networks may persist for a particularly long period after the restoration of colonic mucosa architecture and the regression of colitis.

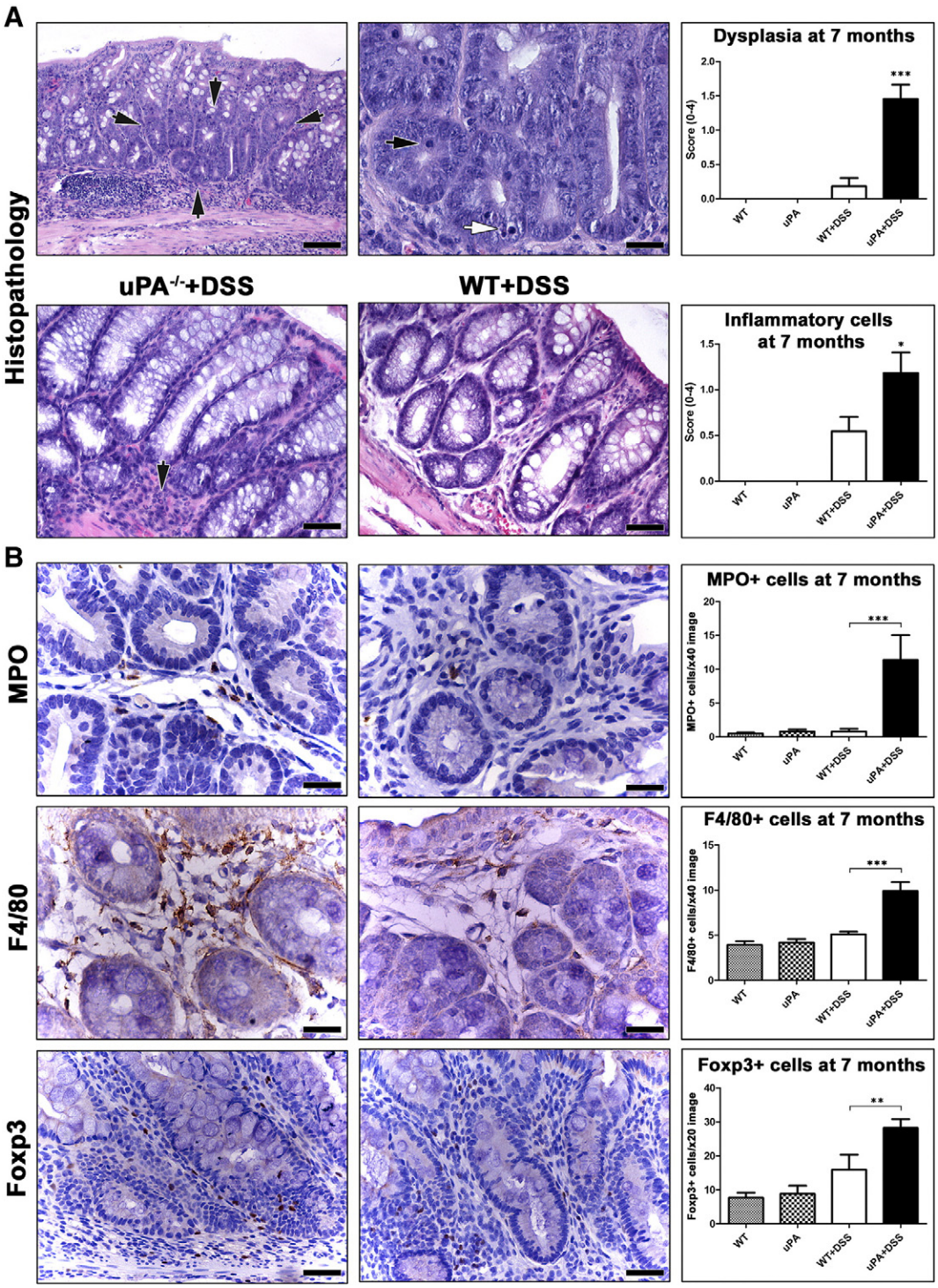

Figure 2. Dysplasia and resident inflammatory cells in the non-neoplastic colonic mucosa of mice at 7 months after DSS treatment. (A) Focal dysplasia in the colonic mucosa of a uPA$^{-/-}$ + DSS mouse (outlined by arrows). Dysplastic glands are readily distinguishable at low power magnification on the basis of their increased cellularity and loss of goblet cells. At higher magnification, the same dysplastic glands show the typical features of LGD including increased proliferation (black arrow) and apoptosis (white arrow). Scores for dysplasia (upper panel) and inflammatory cells (lower panel) were significantly higher in uPA$^{-/-}$ + DSS mice compared to their WT + DSS counterparts. Despite the absence of colitis, resident inflammatory cells (black arrow in the lower left panel) are more in the otherwise normal non-neoplastic, non-dysplastic colonic mucosa of a uPA$^{-/-}$ + DSS mouse compared to a topographically matched area of a WT + DSS mouse (lower right panel). (B) Morphometric counts of immunohistochemically labeled neutrophils (MPO+), macrophages (F4/80+), and Treg (Foxp3+) provide further evidence that the numbers of immune cells in the colonic mucosa of uPA$^{-/-}$ mice do not regress to baseline WT + DSS levels at 7 months after colitogenic insult. Hematoxylin and eosin (A). IHC: DAB chromogen, hematoxylin counterstain (B). Scale bars, 100 μm (A, upper left); 50 μm (A, lower panel and B, Foxp3); 25 μm (A, upper right and B, MPO and F4/80). Numbers on the *y*-axis of bar graphs correspond to the means ± SEM of the histologic parameters assessed; *$P < .05$, **$P < .001$, ***$P < .0001$.

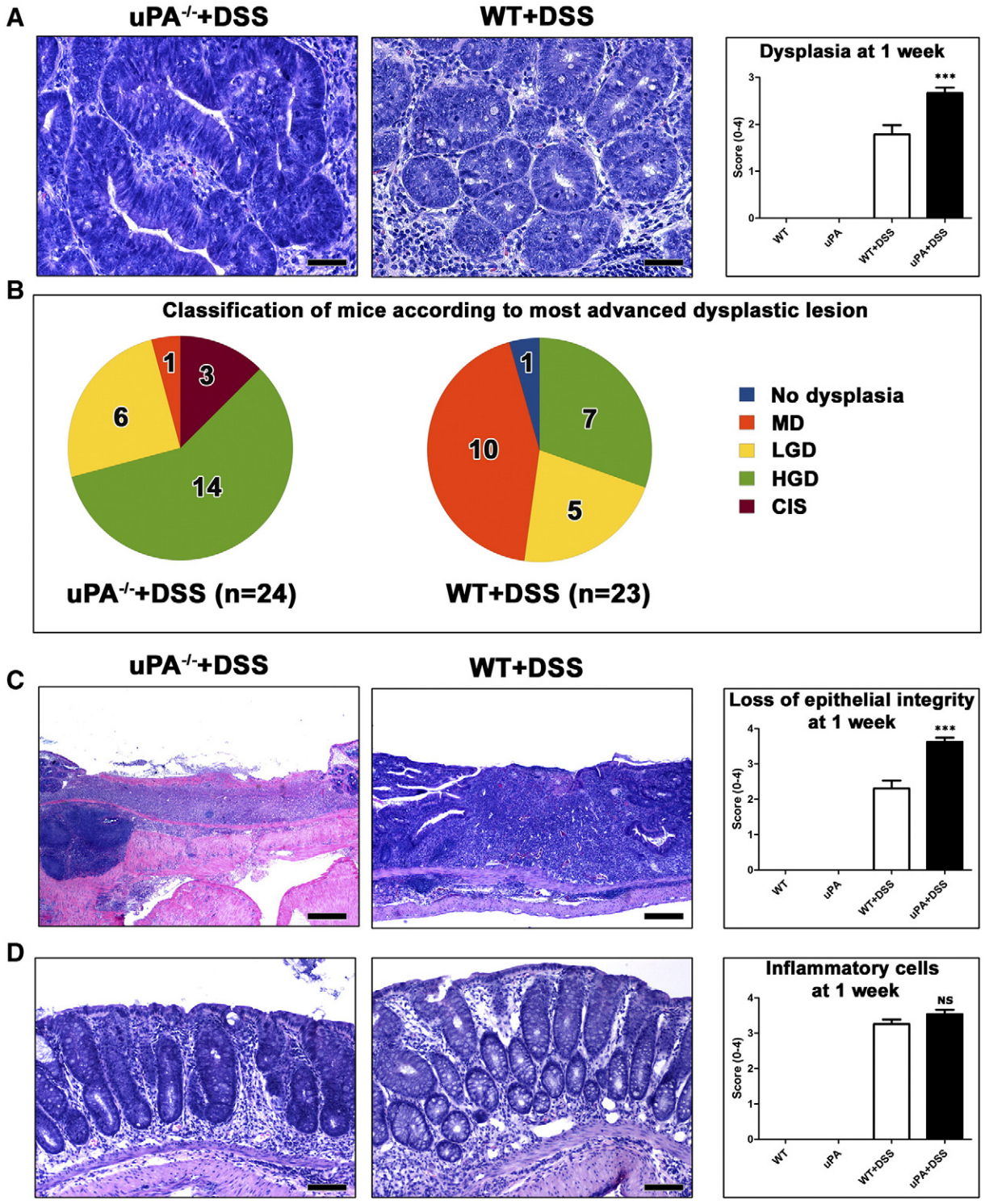

Figure 3. Effects of uPA deficiency in the histopathology of colitis at 1 week after DSS treatment. (A) CIS arising in glands with HGD in uPA$^{-/-}$ + DSS mouse colitis. Typical LGD from a WT + DSS mouse is shown on the side for comparison. Colitis-associated dysplasia scores are significantly raised due to deficiency in uPA. (B) The occurrence of the most advanced grades of dysplasia is higher in uPA$^{-/-}$ mice compared to their WT counterparts. (C) The healing of typical DSS-induced colonic ulcers is retarded due to uPA deficiency. Consequently, the surface epithelium deficit scores are significantly higher in uPA$^{-/-}$ than in WT mice. (D) In non-ulcerated areas of colonic mucosa, uPA$^{-/-}$ and WT mice show comparable amounts of inflammatory cell infiltration. Hematoxylin and eosin (A, C, and D). Scale bars, 50 μm (A); 250 μm (C); 100 μm (D). Numbers on the *y*-axis of bar graphs correspond to the means ± SEM of histologic scores; ***$P < .0001$; NS, $P > .05$.

At 1 Week after DSS Treatment, the Colon of uPA$^{-/-}$ Mice Has More Advanced Dysplastic Lesions

In an effort to explain why uPA$^{-/-}$ + DSS mice develop colonic polypoid adenomas in the long term, while WT + DSS ones do not, we next examined the colon of mice at the early time point of 1 week after DSS treatment. We found that WT and uPA$^{-/-}$ controls showed normal colon histology, whereas their DSS-treated counterparts had the typical DSS-associated ulcerative colitis. At this early time point, DSS-treated mice had numerous foci of epithelial dysplasia, characterized by the same histopathologic and immunohistochemical features as those described in polyps (Figure 3*A*). Colonic dysplastic foci of uPA$^{-/-}$ + DSS mice, however, were in a more advanced stage of the dysplasia/preneoplasia sequence than those of WT + DSS mice (P = .0001; Figure 3, *A* and *B*). A total of 2-minute polyps were found in 2 uPA$^{-/-}$ + DSS mice (2 of 24) and 1-minute polyp was found in the WT + DSS mice (1 of 23). DSS-induced ulcerative lesions, located mostly at the last part of the descending colon and the rectum, consistently presented a larger surface epithelium deficit in the uPA$^{-/-}$ + DSS mice compared to the same lesions of the WT + DSS mice (P < .0001; Figure 3*C*). In the non-ulcerative parts of the gut mucosa, however, colitis in both groups of DSS-treated mice was characterized by comparable levels of inflammatory cell infiltration (P = .1098; Figure 3*D*).

uPA Deficiency Affects the Colitis Inflammatory Cell Component at 1 Week after DSS Treatment

To examine whether the tumor-promoting uPA deficiency is associated with a different inflammatory cell composition of DSS colitis, we labeled *in situ* and then quantified selected critical inflammatory cell types in the colonic mucosa. We found that the numbers of MPO+ neutrophils were significantly higher in both the ulcerative lesions (P = .0052; Figure 4*A*) and the remaining colonic mucosa (P = .0079; Figure W4*A*) of uPA$^{-/-}$ + DSS mice compared to topographically matching areas of WT + DSS mice. The presence of neutrophils was unremarkable in both uPA$^{-/-}$ and WT untreated controls (Figure W4*A*). Likewise, F4/80+ macrophages were significantly more in the non-ulcerated colonic mucosa of the uPA$^{-/-}$ + DSS compared to the WT + DSS mice (P = .0011; Figure 4*B*). CD3+ lymphocytes, however, were less in the ulcerative lesions (P = .0039; Figure 4*C*) and in the colonic lamina propria (P = .0282; Figure W4*B*) of uPA$^{-/-}$ + DSS mice than those counted in the corresponding areas of WT + DSS mice. In contrast, CD3+ lymphocytes were more in the colonic mucosa lymphoid follicles of uPA$^{-/-}$ + DSS mice, albeit in non-statistically significant levels (P = .3642; Figure W4*C*). Although comparable numbers of CD3+ cells were identified in the lamina propria of the normal colonic mucosa of both untreated control groups (Figure 4*C*), the lymphoid follicles of uPA$^{-/-}$ mice had more CD3+ cells than their WT counterparts (P = .041; Figure W4*C*). Having documented these differences in the CD3+ cell colonic mucosa population, we next quantified Foxp3+ Treg in four different areas, including the ulcerative lesions (Figure W4*D*), the lamina propria (Figure 4*D*), and the gut-associated lymphoid tissue (GALT; Figure W4*E*) of the colon and the MLN (Figure 4*E*). The number of Foxp3+ cells was lower in the uPA$^{-/-}$ + DSS compared to the WT + DSS mice, with difference reaching significance only in the lamina propria (P = .0282; Figure 4*D*). Interestingly, in the normal colonic mucosa of the non–DSS-treated controls, the same comparison had the opposite outcome (Figure 4*D*). Specifically, uPA$^{-/-}$ mice had significantly more Treg than their WT counterparts in all areas examined (lamina propria, P = .0204; GALT, P = .0015; MLN, P = .0433; Figures 4*D* and W4, *D* and *E*). Finally, c-kit+ mast cells were practically undetectable both in mice with colitis and in the normal colon of the control groups.

uPA Is Upregulated at 1 Week after DSS Treatment and Its Deficiency Affects the Expression of Cytokines

To confirm previously published results suggesting that uPA is upregulated in DSS colitis, we assessed uPA protein in the colon mucosa of mice by ELISA. As expected, WT + DSS mice had significantly higher levels of uPA than the WT untreated controls (P = .0023; Figure 5*A*). Both groups of uPA$^{-/-}$ mice showed no expression of uPA, thus confirming their genetic deficiency. Having shown that deficiency in uPA affects the inflammatory cell component of DSS colitis, we next quantified the expression of selected cytokines with important roles in colitis-associated colon carcinogenesis by real-time PCR and IHC. We found that the gene expression of the pro-inflammatory cytokines TNF-α (Figure 5*B*) and IL-6 (Figure 5*C*), as well as the anti-inflammatory cytokine IL-10 (Figure 5*D*), was significantly upregulated in uPA$^{-/-}$ + DSS compared to WT + DSS mice (P = .0303, P = .0079, and P = .0082, respectively). With IHC, IL-6+ cells were located at the base of colonic mucosa and within the granular tissue of typical DSS-induced ulcers (Figure 5*E*). Morphometric counts of IL-6+ cells were done in these two areas and were in accordance with real-time PCR quantification of *IL-6* expression. IL-6+ cells were significantly more in uPA$^{-/-}$ + DSS compared to WT + DSS mice in both areas (ulcerative lesions, P = .0022; lamina propria, P = .0042) (Figure 5*E*). Likewise, the pro-inflammatory cytokine IL-17 was also found in higher levels in the colonic mucosa (P = .0065) and the MLN (P = .0015) of uPA$^{-/-}$ + DSS mice by IHC(Figure 5*F*).

The Colon of uPA$^{-/-}$ + DSS Mice Has Low Levels of Active TGF-β1 Protein at 1 Week after DSS Treatment

Since the active extracellular form of TGF-β1 is a downstream product of uPA, we next quantified active TGF-β1 in the colon of mice by ELISA. Untreated uPA$^{-/-}$ had lower levels of active TGF-β1 than untreated WT mice; this difference, however, did not reach statistical significance (P = .2222). However, uPA$^{-/-}$ + DSS mice had significantly lower levels in the colon compared to WT + DSS mice (P = .0079; Figure 6*A*). To exclude that this was due to reduced gene expression, we quantitatively determined colonic *TGF-β1* expression by real-time PCR. We found that colitis in both uPA$^{-/-}$ + DSS and WT + DSS mice was characterized by comparable levels of *TGF-β1* expression (Figure 6*A*). This result was further confirmed by TGF-β1–specific IHC that detects the total of TGF-β1 protein without discriminating the active from the latent form (data not shown). In addition to *TGF-β1*, the expression of other important molecules of the TGF-β1 signaling pathway, such as *TGF-βRII* and *SMAD4*, was also found in comparable levels in both uPA$^{-/-}$ + DSS and WT + DSS mice (Figure 6, *C* and *D*).

Discussion

By inducing chemical chronic colitis in uPA$^{-/-}$ mice, we found that the lack of uPA promotes inflammation-associated colorectal neoplasia. Compared to their WT counterparts, DSS-treated uPA$^{-/-}$ mice had an altered colonic mucosa inflammatory milieu and more advanced epithelial preneoplastic changes that led to the formation of large colonic adenomatous polyps.

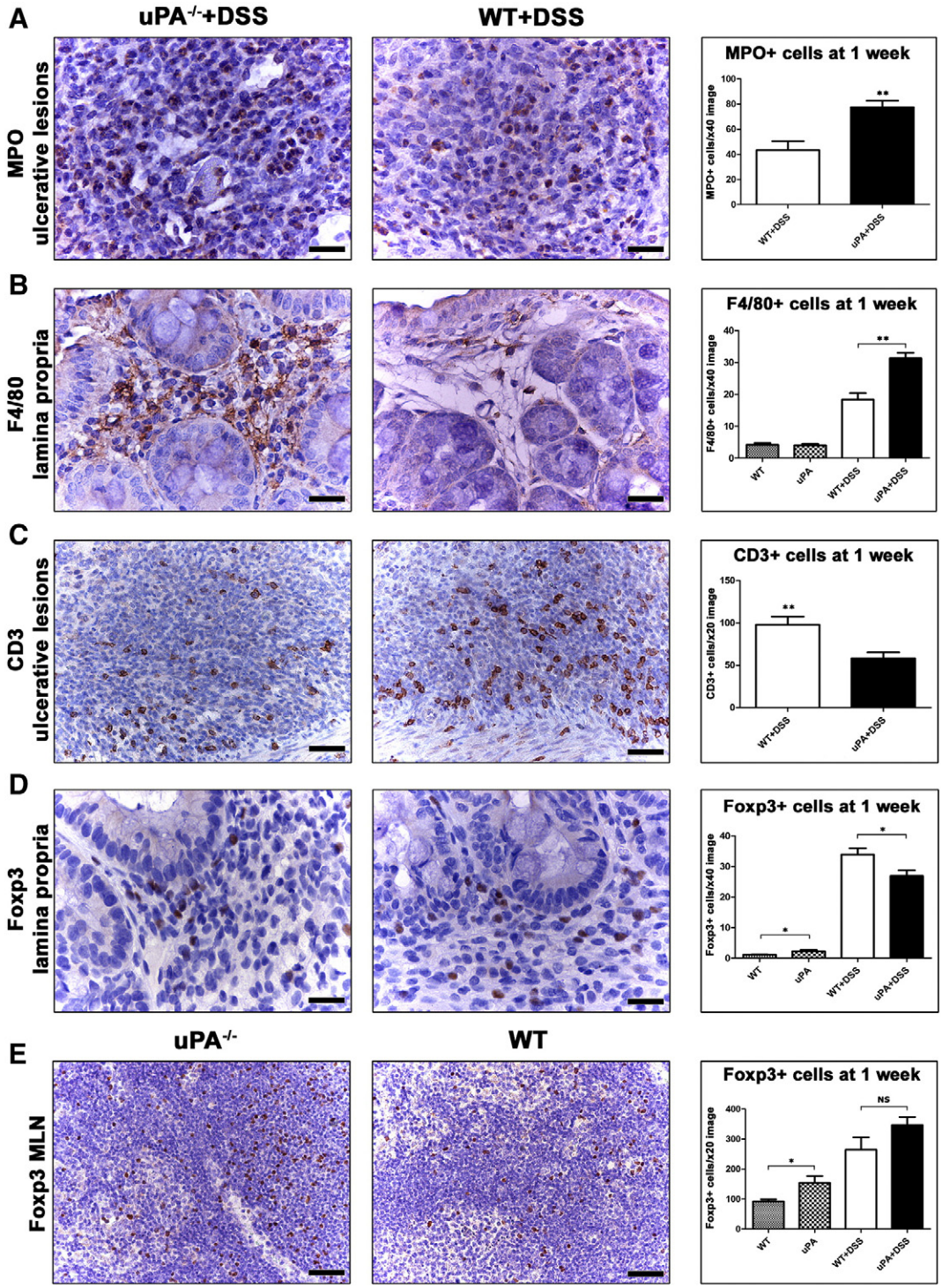

Figure 4. Deficiency in uPA affects the inflammatory cell composition of DSS colitis at 1 week after DSS treatment. (A) Neutrophils (MPO +) in the granular tissue of ulcers and (B) macrophages (F4/80 +) in the lamina propria of colonic mucosa are significantly more in uPA$^{-/-}$ mice. By contrast, numbers of (C) total T-lymphocytes (CD3 +) in colonic ulcers and (D) Treg (Foxp3 +) in the lamina propria are significantly lower due to deficiency in uPA. (E) In the MLN, uPA deficiency correlates with higher numbers of Treg. The difference in Foxp3 + cell counts, however, reaches significance only in the uPA$^{-/-}$ *versus* WT untreated control comparison. IHC: DAB chromogen, hematoxylin counterstain. Scale bars, 25 μm (A, B, and D); 50 μm (C and E). Numbers on the *y*-axis of bar graphs correspond to the mean ± SEM of immunohistochemically positive cell counts; *$P < .05$, **$P < .001$; NS, $P > .05$.

Increased uPA activity in tumors has been clearly associated with poor neoplastic disease prognosis [15]. Consequently, the tumor-promoting role of uPA in neoplastic cell invasion, growth, and metastasis has been extensively studied in many different types of cancer, including colon cancer [15-18,25,26,36]. Except for a few studies reporting on an antiangiogenic tumor-suppressor effect of uPA in human patients [37] and syngeneic orthotopic tumor cell transplant mouse models [37-39], the vast majority of scientific data

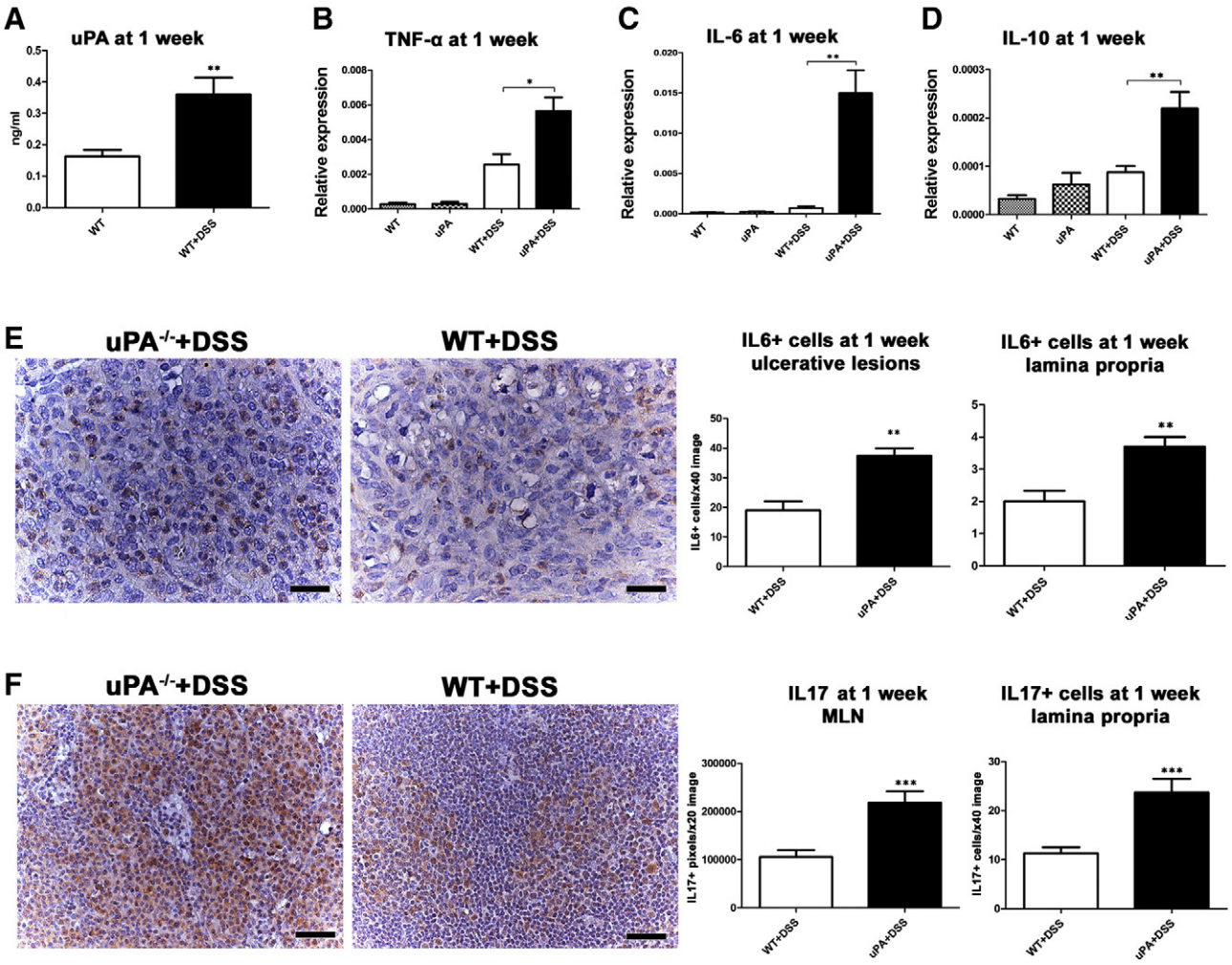

Figure 5. uPA is upregulated and its deficiency affects the cytokine milieu of DSS colitis at 1 week after DSS treatment. (A) uPA protein is significantly upregulated in DSS colitis of WT mice. DSS-treated uPA$^{-/-}$ mice show a significant up-regulation of (B) *TNF-α*, (C) *IL-6*, and (D) *IL-10* in comparison with treatment-matched WT controls. (E) IL-6–specific IHC detects IL-6 + neutrophils in the granular tissue of DSS-induced mucosal ulcers. In these lesions, as well as in the lamina propria of colonic mucosa, significantly more IL-6 + cells were seen in uPA$^{-/-}$ + DSS compared to WT + DSS mice. (F) *In situ* labeling of IL-17 in the MLN of DSS-treated mice. IL-17 is significantly upregulated both in the MLN and in the colonic mucosa of uPA$^{-/-}$ compared to WT control mice. IHC: DAB chromogen, hematoxylin counterstain (E and F). Scale bars, 25 μm (E); 50 μm (F). Numbers on the *y*-axis of bar graphs correspond to the means ± SEM of protein in ng/ml (A); relative cytokine gene expression (B, C, and D) and morphometric counts of IHC-positive pixels or cells (E and F). *$P < .05$, **$P < .001$, ***$P < .0001$.

suggests that uPA confers increased aggressiveness to tumors. For that, uPA is widely accepted as a protease of emerging importance in cancer research [15,17,18]. Yet, its role in the early stages of carcinogenesis has hardly ever been studied, with the exception of one study that used the adenomatous polyposis coli–deficient mouse model (Apc$^{Min/+}$) of intestinal polyposis [22]. In that study, Apc$^{Min/+}$ mice, which also lacked the *uPA* gene, developed less polypoid adenomas than the Apc$^{Min/+}$ controls. uPA deficiency, however, did not affect polyp growth. Furthermore, neoplastic cell proliferation and vascularization were found to be increased in Apc$^{Min/+}$uPA$^{-/-}$ mice [22]. Although these findings agree with our results in that uPA is not essential for the formation of intestinal adenomatous polyps, the basic conclusions regarding the role of uPA in colon carcinogenesis are contradictory. According to that study, the lack of uPA decreased the frequency of polyps in Apc$^{Min/+}$ mice, whereas in our study the lack of uPA led to colitis-associated polyp formation. Fundamental differences between the two mouse models may account for this discrepancy. One important difference is that in our DSS colitis model dysplastic and early neoplastic lesions are caused by inflammation, whereas in the Apc$^{Min/+}$ model such lesions develop in the absence of inflammation, due to an intrinsic defect of the *Wnt* signaling pathway [40]. Interestingly, when Apc$^{Min/+}$uPA$^{-/-}$ mice were treated with DSS for just 1 week, the protection, which was attributed to uPA deficiency, was abolished [22]. This experiment bridges the seemingly contradictory results of the two studies. Taken together, all the above suggest that the lack of uPA enhances colorectal carcinogenesis when the latter arises in an inflammatory cell/factor–rich environment.

In support to that, we also found a higher percentage of uPA$^{-/-}$ + DSS mice bearing foci of dysplastic glands in the colon (excluding polyps) compared to WT + DSS controls at the 7-month time point. The uPA$^{-/-}$ + DSS dysplastic lesions were in a more advanced stage

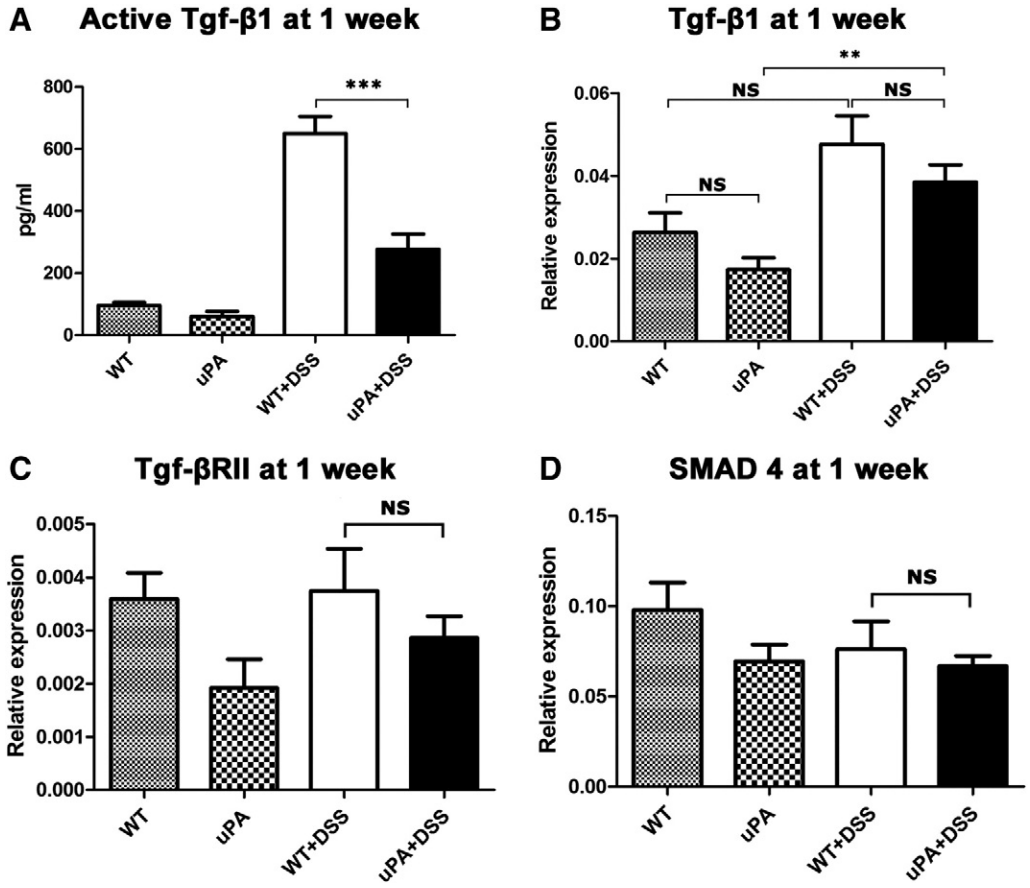

Figure 6. Low levels of active TGF-β1 are found in uPA$^{-/-}$ mouse colitis. (A) Active TGF-β1–specific ELISA reveals that under inflammatory conditions lower levels of active TGF-β1 are being produced in the colonic mucosa of uPA$^{-/-}$ mice. At the gene expression level, however, (B) *TGF-β1* as well as (C) *TGF-βRII* and (D) *SMAD4* remain unaffected by the lack of uPA. Numbers on the *y*-axis of bar graphs correspond to the means ± SEM of protein in ng/ml (A) and relative cytokine gene expression (B, C, and D). *$P < .05$, **$P < .001$, ***$P < .0001$.

(higher grade) compared to the rare mild dysplastic lesions of WT + DSS mice. This observation also points out that the lack of uPA promotes the progression of inflammatory-induced dysplasia to adenoma.

To study the role of uPA in colitis-associated carcinogenesis, we selected to work with the BALB/c strain of mice, which is not susceptible to colorectal carcinogenesis with protocols using DSS alone, i.e., without combining it with carcinogens, such as azoxymethane [41,42]. In addition, this strain, in contrast to C57BL/6 mice, does not develop overt chronic colitis after the initial episodes of acute DSS-induced inflammation [43]. Moreover, the three cycles of 3.5% DSS applied are known not to be sufficient for inducing colon carcinogenesis in genetically intact mice [31]. Swiss-Webster and C57BL/6 mice that are by far the most susceptible strains of mice in that regard need at least four cycles of 5% DSS administration to develop colon dysplasia and adenoma [31,44]. Our experimental setting allowed us to clearly demonstrate that while uPA$^{-/-}$ + DSS mice present sporadic large colonic polypoid adenomas at 7 months after DSS treatment, their WT + DSS counterparts do not. The polyps found arose through the classic dysplasia to colorectal neoplasia sequence, had the typical colonic polypoid adenoma histologic features observed in both humans and mice, and showed evidence of common molecular pathway involvement, including the β-catenin/Wnt and the TGF-β1 [45,46]. For that, we propose the DSS-treated uPA$^{-/-}$ mice as a novel genetically engineered mouse model for studying inflammation-initiated colorectal neoplasmatogenesis.

Selected mouse models of DSS colitis–associated colon cancer have been reported to develop invasive cancer in a low percentage (10-25%) several months past DSS treatment. Cancer in these models arise either from polyps or from flat dysplasia/adenoma lesions [31,47]. This, however, was not the case in our uPA$^{-/-}$ + DSS mouse model. At 7 months past DSS treatments, despite exhaustive histologic sectioning, we found no invasive carcinoma lesions neither in the flat dysplastic lesions nor in the stalk or the submucosa at the base of the polyps. Additional studies on uPA$^{-/-}$ mice using more aggressive DSS treatment protocols or protocols combining DSS with chemical carcinogens may be necessary to reveal whether adenoma lesions are able to evolve to carcinoma or if neoplastic cell invasion is reduced (or even halted) due to uPA deficiency, as other reports suggest [15,18,24,25,36,48].

To further characterize the uPA$^{-/-}$ + DSS mouse model of neoplasia, we probed the topographic distribution of selected inflammatory cell types in the polyps. At 7 months after DSS treatments, polyps existed in the absence of colitis. Presumptively, the polyp-associated inflammatory cells represented the tumor-elicited immune response and were not a remaining component of the DSS-induced colitis. Our group, as well as others, have previously reported on the distribution of immune cells in polyps, using classic mouse models of colon neoplasia, such as the Apc$^{Min/+}$ [34,49-54] and the AOM + DSS model [55-57]. The distribution of neutrophils, macrophages, mast cells, and T-helper lymphocytes, including Treg,

in colonic adenomatous polyps as described in the present study matches the one described in other mouse models [34,49-57] and humans [58,59]. This observation suggests that uPA deficiency does not affect the cellular composition and the distribution of the tumor-associated inflammatory infiltrate of colonic polyps. The demonstration of IL-6 + and IL-17 + inflammatory cells at the base of the polyps supports the recently described roles of these cytokines in tumor promotion [6,7,9,53,60].

Untreated uPA$^{-/-}$ mice showed no evidence of altered colonic histology with increasing age. It is concluded that deficiency in uPA does not affect colonic mucosa homeostasis under normal conditions, at least until the age of 9 months, which was the end point of our study. DSS-challenged uPA$^{-/-}$ mice, with the exception of polypoid adenoma formation and increased colonic gland dysplasia, exhibited a restored colonic architecture and absence of colitis at 7 months after treatment. However, compared to treatment-matched WT mice, they had higher numbers of colonic mucosa resident inflammatory cells, including neutrophils, macrophages, IL-6 + and IL-17 + cells, and Treg. This finding suggests that uPA deficiency correlates with an altered immune response to colitogenic stimuli that persists for a particularly long period. The up-regulation of immune cells, although subtle at 7 months after colitis insults, was somewhat surprising, since uPA$^{-/-}$ mice have been reported to show less inflammatory cells, impairment in both innate and adaptive immunity, and a decreased immune response to infection and tissue injury [22,23,61-63].

To more accurately assess the uPA-associated alterations in the inflammatory response after DSS-induced colonic mucosa injury, we examined the colon of mice at an early time point after DSS treatments, i.e., 1 week after the last DSS cycle. We found that DSS-treated mice presented foci of colonic dysplastic glands, which in the long term have been reported to evolve to neoplasia through a well-characterized sequence of events [33,45,46]. We hypothesized that preneoplastic lesions in the colon of uPA$^{-/-}$ + DSS mice may have thrived and evolved into well-sized polyps due to a particular tumor-promoting inflammatory milieu. At 1 week after DSS treatment, we found that uPA$^{-/-}$ + DSS and WT + DSS mice had numerous dysplastic lesions in comparable numbers. However, uPA deficiency significantly correlated with a more advanced grade of the dysplastic lesions. This finding co-existed with a more robust infiltration of neutrophils and macrophages and an inflammatory response characterized by significantly elevated levels of pro-inflammatory cytokines, such as TNF-α, IL-17, and especially IL-6. The concomitant elevation of the anti-inflammatory cytokine IL-10 was evidently unable to downregulate these inflammatory cells and cytokines, which have been shown to promote carcinogenesis in the colon and other sites [6,7,9,53,64]. The uPA$^{-/-}$ + DSS mouse colitis was also different from the one in WT + DSS mice in that it exhibited less T-lymphocytes in the ulcerative lesions and the remaining colonic lamina propria and more in the organized lymphoid tissue of the bowel. Likewise, the Foxp3 + suppressive subset of T-lymphocytes (Treg) followed a similar pattern. This finding suggests that T-lymphocytes and Treg accumulate in the organized lymphoid bowel tissue and MLN of uPA$^{-/-}$ + DSS mice, but their translocation in the damaged mucosa is retarded. This is probably due to their reduced mobility because of the altered cell–extracellular matrix interactions caused by the lack of uPA-mediated proteolysis [11,61].

Our findings regarding Treg are interesting, given the debated role of this immune-suppressive subset of lymphocytes in carcinogenesis [53,65,66]. Indeed, the roles of Treg in cancer appear paradoxical. Studies correlating high densities of tumor-associated Treg with poor prognosis in several types of human cancers are now challenged by studies on the same types of cancer demonstrating correlation with longer survival of patients [67-72]. Likewise, data from mouse models indicating that Treg, which accumulate in developing tumors, function mainly to suppress protective antineoplastic immune responses [66,73] are challenged by our studies in mice that show that the adoptive transfer of Treg not only protects but is also capable of diminishing already established intestinal, breast, and prostate cancers [33,49-53,64,74]. In the present study, we find that both uPA$^{-/-}$ DSS–treated and untreated mice have significantly more Treg in their GALT compared to their WT controls. This agrees with the results of a recent study that elegantly dissects previously unknown associations of uPA and Treg homeostasis. This study demonstrates that uPA$^{-/-}$ mice are characterized by increased Treg development, yet impaired Treg suppressive function [75]. These results, along with the observations of recent studies, which show that the capacity of Treg to suppress or promote carcinogenesis depends on their activation status [52,67,74], suggest that the impaired function of Treg in uPA$^{-/-}$ mice may, at least in part, contribute to their susceptibility in inflammatory-associated colon carcinogenesis.

This susceptibility, however, may also have another more straightforward explanation. Indeed, uPA$^{-/-}$ + DSS mice had more extensive ulcerative lesions than WT + DSS mice. In the DSS model of colitis, this translates to a more robust inflammatory response, since the delayed restoration of colon epithelial integrity retains the exposure of gut mucosa immune system elements in gut flora antigenic stimuli. The delayed ulcer re-epithelialization of uPA$^{-/-}$ mice observed in our study at 1 week after DSS treatment reflects the decreased wound healing rate of this mouse model [14,76,77]. The profound up-regulation of uPA in the intestines of humans with inflammatory bowel disease [78,79] and DSS-treated rodents [80,81], which was also confirmed in the present study, indicates that uPA is involved in gut mucosa ulcer healing. The full restoration of bowel mucosa architecture at 7 months after DSS-induced injury, despite the occasional presence of some remaining solitary small ulcers in the rectum, suggests that uPA deficiency impairs but not fully hampers the colon mucosa healing capacity in mice.

Given that TGF-β1 extracellular activation depends, in a considerable degree, on uPA proteolytic function [14,27,28], we also assessed selective elements of the TGF-β1 pathway in uPA$^{-/-}$ mice. We found that the gene expression levels of TGF-β1, its receptor TGF-βRII, and the key downstream transcription factor of TGF-β1 signaling SMAD4 [2,29,45] were similar in both uPA$^{-/-}$ + DSS and WT + DSS–treated mice. This finding shows that uPA deficiency does not affect the TGF-β1 pathway at the gene expression level. However, using an ELISA that specifically detects the active form of TGF-β1, we found that uPA deficiency significantly lowered the presence of the extracellular active TGF-β1 in the inflamed colonic mucosa. Untreated uPA$^{-/-}$ mice also had lower levels of active TGF-β1 compared to their WT counterparts, but this difference was not significant and less pronounced compared to the one seen in DSS-treated mice. This indicates that under normal conditions, low levels of active TGF-β1 produced by cleavage of its latent form by other non–uPA-related proteases [28] may suffice for preserving gut health.

Normal TGF-β1 signaling is important in preserving the homeostasis of colonic epithelium and suppressing early neoplasia through antiproliferating signals. At a later stage of neoplastic

evolution, however, TGF-β1 has been shown to promote invasion and metastasis [2,29,45,82]. An intact TGF-β1 is also needed for the appropriate regulation of immune responses and wound healing [83]. Taken together, these data suggest that the inability of uPA$^{-/-}$ mice to produce adequate amounts of the extracellularly cleaved biologically active form of TGF-β1 may have contributed to their increased risk for colon tumorigenesis at many different levels, involving early neoplastic cell evolution, inflammation, and impaired wound healing. This finding also highlights the fact that the studying of the tumorigenic corruptions of the TGF-β1 signaling pathway should not only focus at the gene level but also expand to the extracellular events leading to the generation of the active TGF-β1.

The results of this study challenge the current notion according to which uPA is viewed solely as a tumor promoter. Instead, they suggest that uPA may act as a tumor suppressor in the early stages of inflammation-associated colon carcinogenesis. Importantly, they also show that the lack of a single protease in the environment of colonic epithelial preneoplastic lesions, which develop due to episodes of colitis, may determine whether these lesions will progress to neoplasia in due time.

Acknowledgments

We thank the Bodossaki Foundation for the kind donation of real-time PCR instrumentation.

References

[1] Liotta LA and Kohn EC (2001). The microenvironment of the tumour-host interface. *Nature* **411**, 375–379.
[2] Bissell MJ and Radisky D (2001). Putting tumours in context. *Nat Rev Cancer* **1**, 46–54.
[3] Hanahan D and Weinberg RA (2011). Hallmarks of cancer: the next generation. *Cell* **144**, 646–674.
[4] Hussain SP and Harris CC (2007). Inflammation and cancer: an ancient link with novel potentials. *Int J Cancer* **121**, 2373–2380.
[5] López-Otín C and Matrisian LM (2007). Emerging roles of proteases in tumour suppression. *Nat Rev Cancer* **7**, 800–808.
[6] Mantovani A, Allavena P, Sica A, and Balkwill F (2008). Cancer-related inflammation. *Nature* **454**, 436–444.
[7] Grivennikov SI, Greten FR, and Karin M (2010). Immunity, inflammation, and cancer. *Cell* **140**, 883–899.
[8] Mason SD and Joyce JA (2011). Proteolytic networks in cancer. *Trends Cell Biol* **21**, 228–237.
[9] Terzic J, Grivennikov S, Karin E, and Karin M (2010). Inflammation and colon cancer. *Gastroenterology* **138**, 2101–2114.e5.
[10] Dvorak HF (1986). Tumors: wounds that do not heal. Similarities between tumor stroma generation and wound healing. *N Engl J Med* **315**, 1650–1659.
[11] Vaday GG and Lider O (2000). Extracellular matrix moieties, cytokines, and enzymes: dynamic effects on immune cell behavior and inflammation. *J Leukoc Biol* **67**, 149–159.
[12] Crippa MP (2007). Urokinase-type plasminogen activator. *Int J Biochem Cell Biol* **39**, 690–694.
[13] Del Rosso M, Margheri F, Serrati S, Chilla A, Laurenzana A, and Fibbi G (2011). The urokinase receptor system, a key regulator at the intersection between inflammation, immunity, and coagulation. *Curr Pharm Des* **17**, 1924–1943.
[14] Carmeliet P and Collen D (1998). Development and disease in proteinase-deficient mice: role of the plasminogen, matrix metalloproteinase and coagulation system. *Thromb Res* **91**, 255–285.
[15] Dass K, Ahmad A, Azmi AS, Sarkar SH, and Sarkar FH (2008). Evolving role of uPA/uPAR system in human cancers. *Cancer Treat Rev* **34**, 122–136.
[16] Kwaan HC and McMahon B (2009). The role of plasminogen-plasmin system in cancer. *Cancer Treat Res* **148**, 43–66.
[17] Mekkawy AH, Morris DL, and Pourgholami MH (2009). Urokinase plasminogen activator system as a potential target for cancer therapy. *Future Oncol* **5**, 1487–1499.
[18] Duffy MJ (2004). The urokinase plasminogen activator system: role in malignancy. *Curr Pharm Des* **10**, 39–49.
[19] Gutierrez LS, Schulman A, Brito-Robinson T, Noria F, Ploplis VA, and Castellino FJ (2000). Tumor development is retarded in mice lacking the gene for urokinase-type plasminogen activator or its inhibitor, plasminogen activator inhibitor-1. *Cancer Res* **60**, 5839–5847.
[20] Almholt K, Lund LR, Rygaard J, Nielsen BS, Danø K, Rømer J, and Johnsen M (2005). Reduced metastasis of transgenic mammary cancer in urokinase-deficient mice. *Int J Cancer* **113**, 525–532.
[21] Bugge TH, Lund LR, Kombrinck KK, Nielsen BS, Holmbäck K, Drew AF, Flick MJ, Witte DP, Danø K, and Degen JL (1998). Reduced metastasis of polyoma virus middle T antigen-induced mammary cancer in plasminogen-deficient mice. *Oncogene* **16**, 3097–3104.
[22] Ploplis VA, Tipton H, Menchen H, and Castellino FJ (2007). A urokinase-type plasminogen activator deficiency diminishes the frequency of intestinal adenomas in *Apc$^{Min/+}$* mice. *J Pathol* **213**, 266–274.
[23] Shapiro RL, Duquette JG, Roses DF, Nunes I, Harris MN, Kamino H, Wilson EL, and Rifkin DB (1996). Induction of primary cutaneous melanocytic neoplasms in urokinase-type plasminogen activator (uPA)-deficient and wild-type mice: cellular blue nevi invade but do not progress to malignant melanoma in uPA-deficient animals. *Cancer Res* **56**, 3597–3604.
[24] Xie C, Jiang XH, Zhang JT, Sun TT, Dong JD, Sanders AJ, Diao RY, Wang Y, Fok KL, and Tsang LL, et al (2013). CFTR suppresses tumor progression through miR-193b targeting urokinase plasminogen activator (uPA) in prostate cancer. *Oncogene* **32**, 2282–2291 2291.e1–7.
[25] Minoo P, Baker K, Baumhoer D, Terracciano L, Lugli A, and Zlobec I (2010). Urokinase-type plasminogen activator is a marker of aggressive phenotype and an independent prognostic factor in mismatch repair-proficient colorectal cancer. *Hum Pathol* **41**, 70–78.
[26] Halamkova J, Kiss I, Pavlovsky Z, Tomasek J, Jarkovsky J, Cech Z, Tucek S, Hanakova L, Moulis M, and Zavrelova J, et al (2011). Clinical significance of the plasminogen activator system in relation to grade of tumor and treatment response in colorectal carcinoma patients. *Neoplasma* **58**, 377–385.
[27] Lyons RM, Gentry LE, Purchio AF, and Moses HL (1990). Mechanism of activation of latent recombinant transforming growth factor β1 by plasmin. *J Cell Biol* **110**, 1361–1367.
[28] Hyytiainen M, Penttinen C, and Keski-Oja J (2004). Latent TGF-β binding proteins: extracellular matrix association and roles in TGF-β activation. *Crit Rev Clin Lab Sci* **41**, 233–264.
[29] Ikushima Hand Miyazono K (2010). TGFβ signalling: a complex web in cancer progression. *Nat Rev Cancer* **10**, 415–424.
[30] Bierie Band Moses HL (2006). Tumour microenvironment: TGFβ: the molecular Jekyll and Hyde of cancer. *Nat Rev Cancer* **6**, 506–520.
[31] Clapper ML, Cooper HS, and Chang WC (2007). Dextran sulfate sodium-induced colitis-associated neoplasia: a promising model for the development of chemopreventive interventions. *Acta Pharmacol Sin* **28**, 1450–1459.
[32] Poutahidis T, Doulberis M, Karamanavi E, Angelopoulou K, Koutinas CK, and Papazoglou LG (2008). Primary gastric choriocarcinoma in a dog. *J Comp Pathol* **139**, 146–150.
[33] Erdman SE, Poutahidis T, Tomczak M, Rogers AB, Cormier K, Plank B, Horwitz BH, and Fox JG (2003). CD4$^+$ CD25$^+$ regulatory T lymphocytes inhibit microbially induced colon cancer in Rag2-deficient mice. *Am J Pathol* **162**, 691–702.
[34] Rao VP, Poutahidis T, Ge Z, Nambiar PR, Horwitz BH, Fox JG, and Erdman SE (2006). Proinflammatory CD4$^+$ CD45RB^{hi} lymphocytes promote mammary and intestinal carcinogenesis in *Apc$^{min/+}$* mice. *Cancer Res* **66**, 57–61.
[35] Pfaffl MW (2001). A new mathematical model for relative quantification in real-time RT-PCR. *Nucleic Acids Res* **29**, e45.
[36] Berger DH (2002). Plasmin/plasminogen system in colorectal cancer. *World J Surg* **26**, 767–771.
[37] Merchan JR, Chan B, Kale S, Schnipper LE, and Sukhatme VP (2003). In vitro and in vivo induction of antiangiogenic activity by plasminogen activators and captopril. *J Natl Cancer Inst* **95**, 388–399.
[38] Merchan JR, Tang J, Hu G, Lin Y, Mutter W, Tong C, Karumanchi SA, Russell SJ, and Sukhatme VP (2006). Protease activity of urokinase and tumor progression in a syngeneic mammary cancer model. *J Natl Cancer Inst* **98**, 756–764.
[39] Zhang J, Sud S, Mizutani K, Gyetko MR, and Pienta KJ (2011). Activation of urokinase plasminogen activator and its receptor axis is essential for macrophage infiltration in a prostate cancer mouse model. *Neoplasia* **13**, 23–30.

[40] Moser AR, Luongo C, Gould KA, McNeley MK, Shoemaker AR, and Dove WF (1995). ApcMin: a mouse model for intestinal and mammary tumorigenesis. *Eur J Cancer* **31A**, 1061–1064.

[41] Suzuki R, Kohno H, Sugie S, Nakagama H, and Tanaka T (2006). Strain differences in the susceptibility to azoxymethane and dextran sodium sulfate-induced colon carcinogenesis in mice. *Carcinogenesis* **27**, 162–169.

[42] Gao Y, Li X, Yang M, Zhao Q, Liu X, Wang G, Lu X, Wu Q, Wu J, and Yang Y, et al (2013). Colitis-accelerated colorectal cancer and metabolic dysregulation in a mouse model. *Carcinogenesis* **34**, 1861–1869.

[43] Melgar S, Karlsson A, and Michaelsson E (2005). Acute colitis induced by dextran sulfate sodium progresses to chronicity in C57BL/6 but not in BALB/c mice: correlation between symptoms and inflammation. *Am J Physiol Gastrointest Liver Physiol* **288**, G1328–G1338.

[44] Cooper HS, Murthy S, Kido K, Yoshitake H, and Flanigan A (2000). Dysplasia and cancer in the dextran sulfate sodium mouse colitis model. relevance to colitis-associated neoplasia in the human: a study of histopathology, B-catenin and p53 expression and the role of inflammation. *Carcinogenesis* **21**, 757–768.

[45] Boivin GP, Washington K, Yang K, Ward JM, Pretlow TP, Russell R, Besselsen DG, Godfrey VL, Doetschman T, and Dove WF, et al (2003). Pathology of mouse models of intestinal cancer: consensus report and recommendations. *Gastroenterology* **124**, 762–777.

[46] Riddell RH (2003). Tumors of the intestines. Washington, DC: Armed Forces Institute of Pathology; 2003.

[47] Okayasu I, Yamada M, Mikami T, Yoshida T, Kanno J, and Ohkusa T (2002). Dysplasia and carcinoma development in a repeated dextran sulfate sodium-induced colitis model. *J Gastroenterol Hepatol* **17**, 1078–1083.

[48] Markl B, Renk I, Oruzio DV, Jähnig H, Schenkirsch G, Scholer C, Ehret W, Arnholdt HM, Anthuber M, and Spatz H (2010). Tumour budding, uPA and PAI-1 are associated with aggressive behaviour in colon cancer. *J Surg Oncol* **102**, 235–241.

[49] Poutahidis T, Rao VP, Olipitz W, Taylor CL, Jackson EA, Levkovich T, Lee CW, Fox JG, Ge Z, and Erdman SE (2009). CD4+ lymphocytes modulate prostate cancer progression in mice. *Int J Cancer* **125**, 868–878.

[50] Erdman SE, Sohn JJ, Rao VP, Nambiar PR, Ge Z, Fox JG, and Schauer DB (2005). $CD4^+CD25^+$ regulatory lymphocytes induce regression of intestinal tumors in $Apc^{Min/+}$ mice. *Cancer Res* **65**, 3998–4004.

[51] Rao VP, Poutahidis T, Ge Z, Nambiar PR, Boussahmain C, Wang YY, Horwitz BH, Fox JG, and Erdman SE (2006). Innate immune inflammatory response against enteric bacteria *Helicobacter hepaticus* induces mammary adenocarcinoma in mice. *Cancer Res* **66**, 7395–7400.

[52] Erdman SE, Rao VP, Olipitz W, Taylor CL, Jackson EA, Levkovich T, Lee CW, Horwitz BH, Fox JG, and Ge Z, et al (2010). Unifying roles for regulatory T cells and inflammation in cancer. *Int J Cancer* **126**, 1651–1665.

[53] Erdman SE and Poutahidis T (2010). Roles for inflammation and regulatory T cells in colon cancer. *Toxicol Pathol* **38**, 76–87.

[54] McClellan JL, Davis JM, Steiner JL, Enos RT, Jung SH, Carson JA, Pena MM, Carnevale KA, Berger FG, and Murphy EA (2012). Linking tumor-associated macrophages, inflammation, and intestinal tumorigenesis: role of MCP-1. *Am J Physiol Gastrointest Liver Physiol* **303**, G1087–G1095.

[55] Tanaka T, Kohno H, Suzuki R, Yamada Y, Sugie S, and Mori H (2003). A novel inflammation-related mouse colon carcinogenesis model induced by azoxymethane and dextran sodium sulfate. *Cancer Sci* **94**, 965–973.

[56] Shang K, Bai YP, Wang C, Wang Z, Gu HY, Du X, Zhou XY, Zheng CL, Chi YY, and Mukaida N, et al (2012). Crucial involvement of tumor-associated neutrophils in the regulation of chronic colitis-associated carcinogenesis in mice. *PLoS One* **7**, e51848.

[57] Fukata M, Hernandez Y, Conduah D, Cohen J, Chen A, Breglio K, Goo T, Hsu D, Xu R, and Abreu MT (2009). Innate immune signaling by toll-like receptor-4 (TLR4) shapes the inflammatory microenvironment in colitis-associated tumors. *Inflamm Bowel Dis* **15**, 997–1006.

[58] McLean MH, Murray GI, Stewart KN, Norrie G, Mayer C, Hold GL, Thomson J, Fyfe N, Hope M, and Mowat NA, et al (2011). The inflammatory microenvironment in colorectal neoplasia. *PLoS One* **6**, e15366.

[59] Pages F, Galon J, and Fridman WH (2008). The essential role of the in situ immune reaction in human colorectal cancer. *J Leukoc Biol* **84**, 981–987.

[60] Naugler WE and Karin M (2008). The wolf in sheep's clothing: the role of interleukin-6 in immunity, inflammation and cancer. *Trends Mol Med* **14**, 109–119.

[61] Beck JM, Preston AM, and Gyetko MR (1999). Urokinase-type plasminogen activator in inflammatory cell recruitment and host defense against pneumocystis carinii in mice. *Infect Immun* **67**, 879–884.

[62] Gyetko MR, Sud S, and Chensue SW (2004). Urokinase-deficient mice fail to generate a type 2 immune response following schistosomal antigen challenge. *Infect Immun* **72**, 461–467.

[63] Deindl E, Ziegelhoffer T, Kanse SM, Fernandez B, Neubauer E, Carmeliet P, Preissner KT, and Schaper W (2003). Receptor-independent role of the urokinase-type plasminogen activator during arteriogenesis. *FASEB J* **17**, 1174–1176.

[64] Poutahidis T, Haigis KM, Rao VP, Nambiar PR, Taylor CL, Ge Z, Watanabe K, Davidson A, Horwitz BH, and Fox JG, et al (2007). Rapid reversal of interleukin-6-dependent epithelial invasion in a mouse model of microbially induced colon carcinoma. *Carcinogenesis* **28**, 2614–2623.

[65] Fuchs T and Allgayer H (2003). Transcriptional regulation of the urokinase receptor (u-PAR)—a central molecule of invasion and metastasis. *Biol Chem* **384**, 755–761.

[66] Zou W (2006). Regulatory T cells, tumour immunity and immunotherapy. *Nat Rev Immunol* **6**, 295–307.

[67] Whiteside TL (2012). What are regulatory T cells (treg) regulating in cancer and why? *Semin Cancer Biol* **22**, 327–334.

[68] Curiel TJ, Coukos G, Zou L, Alvarez X, Cheng P, Mottram P, Evdemon-Hogan M, Conejo-Garcia JR, Zhang L, and Burow M, et al (2004). Specific recruitment of regulatory T cells in ovarian carcinoma fosters immune privilege and predicts reduced survival. *Nat Med* **10**, 942–949.

[69] Leffers N, Gooden MJ, de Jong RA, Hoogeboom BN, ten Hoor KA, Hollema H, Boezen HM, van der Zee AG, Daemen T, and Nijman HW (2009). Prognostic significance of tumor-infiltrating T-lymphocytes in primary and metastatic lesions of advanced stage ovarian cancer. *Cancer Immunol Immunother* **58**, 449–459.

[70] Wilke CM, Wu K, Zhao E, Wang G, and Zou W (2010). Prognostic significance of regulatory T cells in tumor. *Int J Cancer* **127**, 748–758.

[71] Salama P, Phillips M, Grieu F, Morris M, Zeps N, Joseph D, Platell C, and Iacopetta B (2009). Tumor-infiltrating $FOXP3^+$ T regulatory cells show strong prognostic significance in colorectal cancer. *J Clin Oncol* **27**, 186–192.

[72] Badoual C, Hans S, Fridman WH, Brasnu D, Erdman S, and Tartour E (2009). Revisiting the prognostic value of regulatory T cells in patients with cancer. *J Clin Oncol* **27**, e5–e6 Author reply e7.

[73] Gallimore A and Godkin A (2008). Regulatory T cells and tumour immunity—observations in mice and men. *Immunology* **123**, 157–163.

[74] Erdman SE and Poutahidis T (2010). Cancer inflammation and regulatory T cells. *Int J Cancer* **127**, 768–779.

[75] He F, Chen H, Probst-Kepper M, Geffers R, Eifes S, Del Sol A, Schughart K, Zeng AP, and Balling R (2012). PLAU inferred from a correlation network is critical for suppressor function of regulatory T cells. *Mol Syst Biol* **8**, 624.

[76] Jogi A, Rønø B, Lund IK, Nielsen BS, Ploug M, Høyer-Hansen G, Rømer J, and Lund LR (2010). Neutralisation of uPA with a monoclonal antibody reduces plasmin formation and delays skin wound healing in tPA-deficient mice. *PLoS One* **5**, e12746.

[77] Lund LR, Green KA, Stoop AA, Ploug M, Almholt K, Lilla J, Nielsen BS, Christensen IJ, Craik CS, and Werb Z, et al (2006). Plasminogen activation independent of uPA and tPA maintains wound healing in gene-deficient mice. *EMBO J* **25**, 2686–2697.

[78] Gibson PR, van de Pol E, and Doe WF (1991). Cell associated urokinase activity and colonic epithelial cells in health and disease. *Gut* **32**, 191–195.

[79] de Bruin PA, Crama-Bohbouth G, Verspaget HW, Verheijen JH, Dooijewaard G, Weterman IT, and Lamers CB (1988). Plasminogen activators in the intestine of patients with inflammatory bowel disease. *Thromb Haemost* **60**, 262–266.

[80] Crott JW, Choi SW, Ordovas JM, Ditelberg JS, and Mason JB (2004). Effects of dietary folate and aging on gene expression in the colonic mucosa of rats: implications for carcinogenesis. *Carcinogenesis* **25**, 69–76.

[81] Rivera E, Flores I, Rivera E, and Appleyard CB (2006). Molecular profiling of a rat model of colitis: validation of known inflammatory genes and identification of novel disease-associated targets. *Inflamm Bowel Dis* **12**, 950–966.

[82] Elliott RL and Blobe GC (2005). Role of transforming growth factor beta in human cancer. *J Clin Oncol* **23**, 2078–2093.

[83] Prud'homme GJ (2007). Pathobiology of transforming growth factor β in cancer, fibrosis and immunologic disease, and therapeutic considerations. *Lab Invest* **87**, 1077–1091.

Supplementary materials

Table W1. Primers Used for Gene Expression Analysis.

Primer	Sequence (5′-3′)	Positions [1]	Amplicon Size (bp)
TNF-α (F)	ACGTCGTAGCAAACCACCAA	437-456	146
TNF-α (R)	GAGAACCTGGGAGTAGACAAGG	561-582	
IL-6 (F)	GGATACCACTCCCAACAGACC	142-162	144
IL-6 (R)	TCTGCAAGTGCATCATCG	268-285	
IL-10 (F)	TTCCCTGGGTGAGAAGCTGAA	405-425	140
IL-10 (R)	CCTTGTAGACACCTTGGTCTTGG	522-544	
TGF-β1 (F)	GGAGAGCCCTGGATACCAAC	1697-1716	149
TGF-β1 (R)	GCAGGGTCCCAGACAGAAG	1810-1829	
SMAD4 (F)	CCATATCACTATGAGCGGGTTG	828-849	144
SMAD4 (R)	CGAATGTCCTTCAGTGGGTAAG	950-971	
TGF-βRII (F)	CTTGCGACAACCAGAAGTCC	580-599	131
TGF-βRII (R)	GTCGTGGCAAACCGTCTC	693-710	
GAPDH (F)	TGTGTCCGTCGTGGATCTGA	761-780	150
GAPDH (R)	TTGCTGTTGAAGTCGCAGGAG	890-910	

[1] According to gene sequences with the following GenBank Accession Nos.: *TNF-α*—NM_013693, *IL6*—NM_031168, *IL10*—NM_010548, *TGF-β1*—NM_011577, *SMAD4*—NM_008540, *TGF-βRII*—NM_009371, *GAPDH*—NM_008084.

Table W2. Concentrations and annealing temperatures of the primers used for gene expression analysis.

Gene	*C* (nM)	*T* (ºC)
TNF-α	300	59
IL-6	250	57
IL-10	150	63
TGF-β	250	59
SMAD4	250	61
TGF-βRII	250	60
GAPDH	300	62

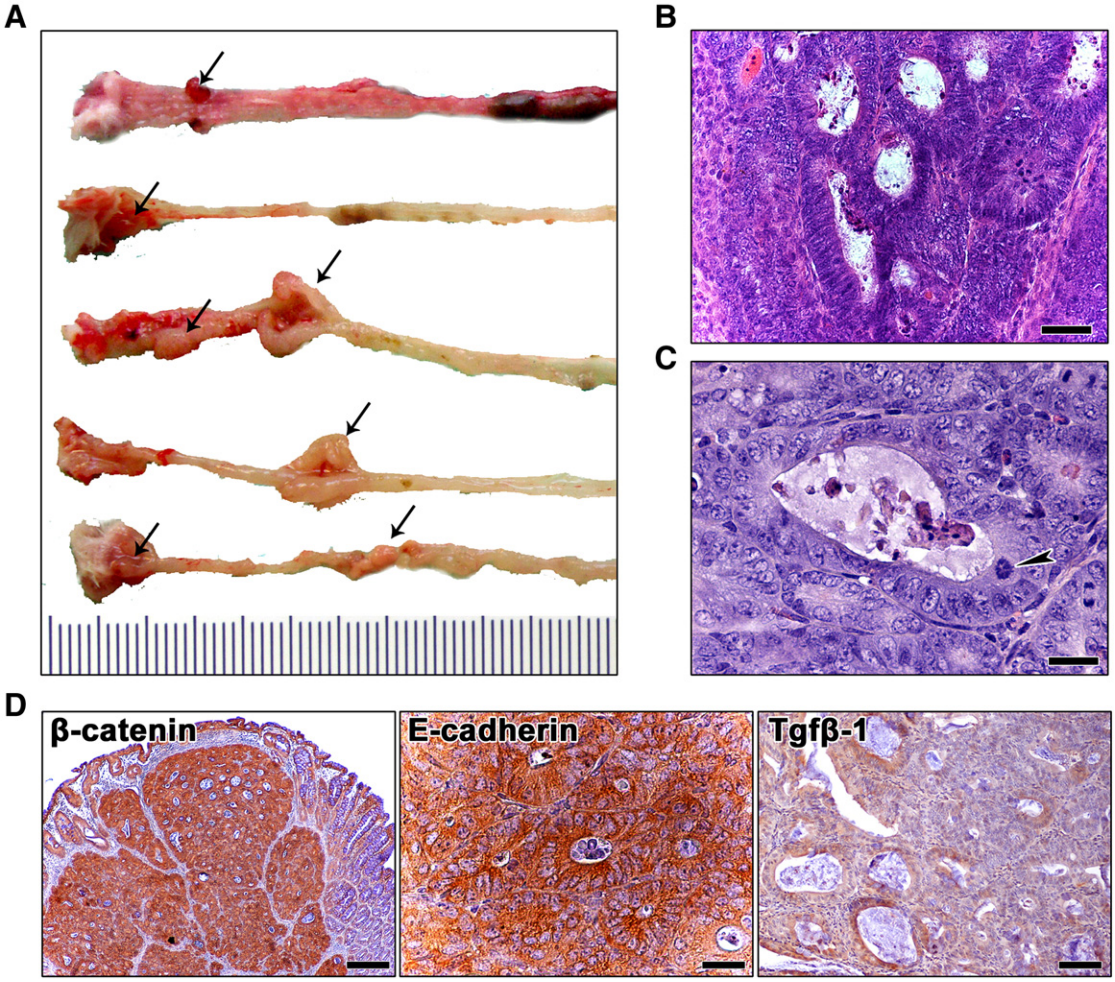

Figure W1. Pathologic features of the uPA$^{-/-}$ + DSS–treated mouse model of colorectal neoplasia. (A) Macroscopic appearance of the seven mouse polyps found in the uPA$^{-/-}$ + DSS experimental group. HGD in polypoid adenomas is typified by (B) back-to-back positioning of angular glands that differ in size and shape, marked pseudostratification of neoplastic epithelia, loss of epithelial cell nuclear polarity, numerous mitotic figures, and (C) nuclear pleomorphism and abnormal mitoses (arrow). (D) β-Catenin abnormal staining patterns sharply demarcate neoplastic glands in a colonic polyp. Neoplastic epithelia also show abnormal cytoplasmic stabilization of E-cadherin and increase or loss of TGF-β1 expression. Hematoxylin and eosin (B and C). IHC: DAB chromogen, hematoxylin counterstain (D). Scale bars, 50 μm (B and D; E-cadherin); 25 μm (C); 100 μm (D; β-catenin and TGF-β1).

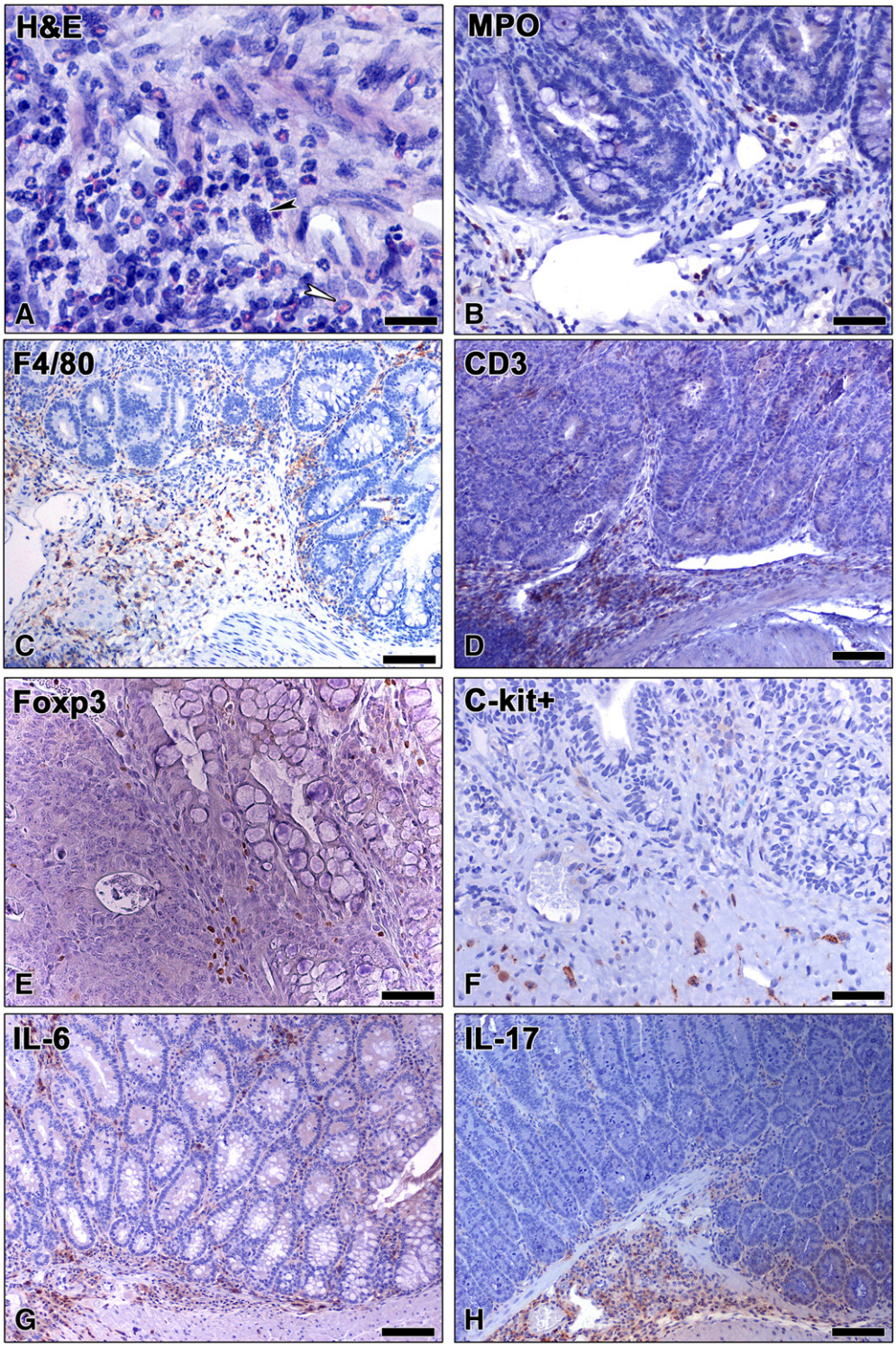

Figure W2. Aspects of the topographic distribution of inflammatory cells in the uPA$^{-/-}$ + DSS mouse polyps. (A) Dense inflammatory infiltrate at the base of a mouse polyp consisting of all types of different immune cells, including mast cells (black arrowhead) and myeloid precursor cells (white arrowhead). Immune cell–specific IHC is used to demonstrate MPO + neutrophils (B), F4/80 + macrophages (C), CD3 + lymphocytes (D), c-kit–positive mast cells (F), and IL-6 + (G) and IL-17 + (H) cells at the base of the mouse polyps. A Foxp3 + Treg infiltrate located at the lateral margins of the neoplastic tissue is also shown (E). Hematoxylin and eosin (A). IHC: DAB chromogen, hematoxylin counterstain (B–H). Scale bars, 25 μm (A); 100 μm (B–D, G, and H); 50 μm (E and F).

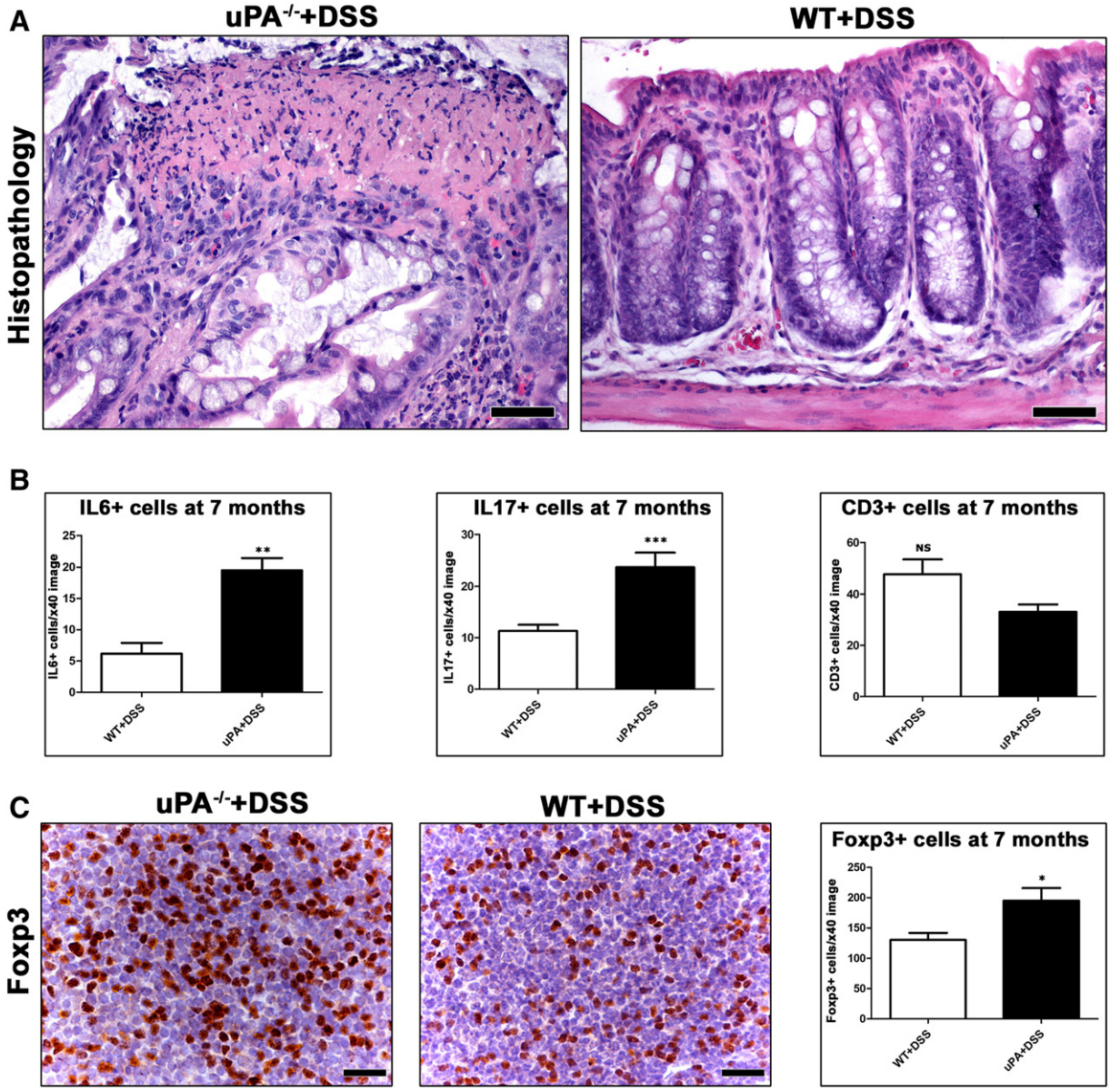

Figure W3. Histopathologic features of mouse colon and immune cell counts of DSS-treated groups at 7 months after DSS treatment. (A) Residual ulcerative lesions with necrotic tissue debris on the surface persist in the rectum of DSS-treated uPA$^{-/-}$ mice. WT mice at 7 months after the last cycle of DSS administration show a completely restored rectal mucosa architecture. (B) Morphometric immune cell count comparison in the lamina propria of colonic mucosa. DSS-treated uPA$^{-/-}$ mice have significantly more IL-6 + and IL-17 + cells compared to WT + DSS mice. CD3 + cells are less in uPA$^{-/-}$ mice, although the difference from the WT controls is not statistically significant. (C) The MLN of the uPA$^{-/-}$ mice bear significantly higher numbers of Foxp3 + Treg. Hematoxylin and eosin (A). IHC: DAB chromogen, hematoxylin counterstain (C). Scale bars, 50 μm (A); 25 μm (C). Numbers on the *y*-axis of bar graphs correspond to the means ± SEM of cell counts.

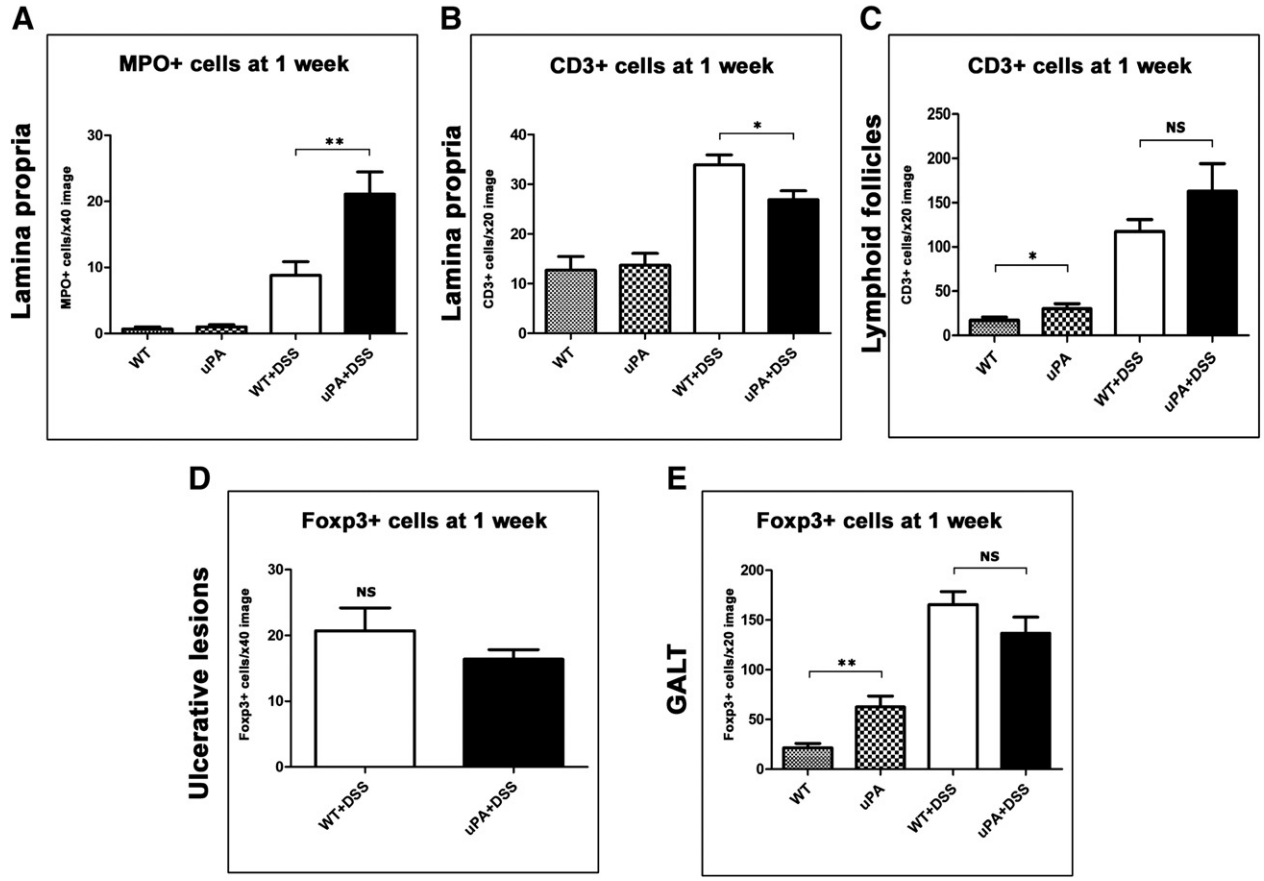

Figure W4. Immune cell counts in the colon of mice at 1 week after DSS treatment. In the lamina propria of colonic mucosa, $uPA^{-/-}$ + DSS mice have more (A) neutrophils (MPO +) and (B) less T-lymphocytes (CD3 +) in comparison with WT + DSS mice. (C) In mucosal lymphoid follicles, uPA deficiency associates with increased numbers of T-lymphocytes in both DSS-treated and non-treated group comparisons. (D) Foxp3 + Treg counts in ulcerative lesions and (E) GALT yield a non-statistically significant difference between $uPA^{-/-}$ + DSS and WT + DSS mice. $uPA^{-/-}$ untreated control mice, however, have significantly more Treg than the WT untreated mice in the GALT. Numbers on the *y*-axis of bar graphs correspond to the means ± SEM of cell counts.